ISRN LUTMDN/TMHP--13/5294—SE
ISSN 0282-1990

Dynamic modeling of a parabolic trough solar power plant

Robert Österholm

Thesis for the Degree of Master of Science

Division of Thermal Power Engineering
Department of Energy Sciences
Faculty of Engineering, LTH
Lund University
P.O. Box 118
SE-221 00 Lund
Sweden

1 ABSTRACT

Models for dynamic simulation of a parabolic trough concentrating solar power plant were developed in Modelica for the simulation software Dymola. The parabolic trough power plant has a two-tank indirect thermal storage with solar salt for the ability to dispatch electric power later in the evening and during the night when little or no solar irradiation is present. The complete system consists of models for incoming solar irradiation, a parabolic trough collector field, thermal storage and a simplified Rankine cycle. A parabolic trough power plant named Andasol located in Aldeire y La Calahorra, Spain, is chosen as a reference system when the complete system model is designed and built in Dymola. The system model is later validated against performance numbers from this reference system in order to make sure a correct implementation has been made. The collector and solar model have also been validated against different papers regarding solar collector performance and show good results.

Finally the system in Dymola has been simulated during a day for different parts of the year with solar data from the same region as the Andasol power plant. The results from these simulations show similarities to how the Andasol power plant operates and how well the system performs under different solar irradiance conditions.

By modeling the system dynamically the changes in insolation over time can be studied to gain information about how it affects the system model in detail. Plant startup time and how long the system can be running on the thermal storage is other parameters that could be studied with this dynamic model.

2 PREFACE

This master thesis will mark the end of my studies in mechanical engineering with specialization in energy. It focuses on dynamic modelling of a thermal solar power plant in a software called Dymola and is conducted together with Modelon AB, Lund, Sweden and the division of thermal power engineering at the department of energy sciences at Lunds tekniska högskola, Lund, Sweden.

3 TABLE OF CONTENT

CONTENTS

4 DISPOSITION

4.1 SHORT BACKGROUND

The initiative to this master thesis was taken by Modelon AB in Lund, Sweden which develop libraries and models for Dymola. They wanted to be able to present the possibilities of using Dymola for customers in the thermal solar business. By developing a set of solar power specific components a complete concentrating solar power plant system can be built fast and simulated dynamically for testing of different control strategies, system configurations and varying solar conditions.

4.2 TASKS AND PURPOSE

The purpose of this thesis is to show the possibilities to dynamically simulate a thermal solar power plant in Dymola. The work will be conducted together with Modelon AB. Tasks will consist of implementing different thermal solar power specific components in Modelica and build complete system models of a concentrating solar power plant which will be simulated for different scenarios. The simulations will be evaluated with data from an existing thermal solar power plant in order to make sure that the models are working and behaving correctly.

5 METHODS

5.1 TOOLS FOR SOLVING THE PROBLEM

This master thesis is based on modelling in a software suite called Dymola, Dynamic Modeling Laboratory. Dymola is developed by Dynasim AB located in Lund and owned by Dassault, France. Dymola is essentially an acausal equation solver for complex systems in a broad field of disciplines like mechanics, electrics and thermodynamics. A system consists of different components that are mathematical interpretations of its physical properties. The models are built using the Modelica object-oriented, declarative, multi-domain modeling language. Dymola then solves the equations over time to generate a dynamic result. As an example heat transferred in a heat exchanger can be solved for a period of time. When the simulation is done the heat transferred can be plotted against the time and the user can quickly study the effects of heat transfer when changes in the system are made. In this case the software will mainly be used to model thermodynamic behavior of a concentrating solar power plant. The models also include some mechanical components like valves and pumps and some control units for these components.

6 INTRODUCTION TO THERMAL SOLAR POWER

6.1 SYSTEM DESCRIPTION

Thermal solar power is a technology of which the solar irradiation on earth is harvested in order to produce power in the range of village type application of 10 kilowatts all the way up to grid connected power plants producing several hundred megawatts. It's an environmentally friendly way of producing power not contributing to the rising amount of greenhouse gases and other hazardous particles that is let out in the atmosphere by other power producing techniques like coal, gas and oil fired power plants.

The basic technique is to concentrate the solar irradiation using a configuration of mirrors to produce high temperature heat. The heat is then transported to a boiler where steam is produced for a steam turbine or the heat is used to power a heat engine. The turbine or heat engine coupled with a generator is then producing electrical power. Some system also has the capability to store heat for use during cloudy days or cloudy parts of the day and through the night. There is a range of different configurations both in the way solar irradiation is concentrated and how the produced heat is used to generate power. The most common, in regards of development and number of units built, thermal solar power plants will be presented later on in this report.

A thermal solar power plant can be divided into three parts consisting of the collector, the thermal storage and the power cycle. Another important part of the system is the media that is used to transport heat from the collector to the power cycle and used to store thermal energy in the thermal storage. The different parts and the most common thermal media used in a typical thermal concentrating solar power plant will be presented and explained in detail below.

6.1.1 Collector

The concentrating device of a thermal solar power plant consists of mirrors focusing the incoming solar irradiation on to a heat absorbing device of some kind. This is done because the solar irradiation per square meter on earth is too small to heat anything to a desired temperature used in power generating applications. By concentrating the irradiation from a large area on to a small point high temperatures can be reached. [1]

The arrangement of the mirrors differs depending on which type of thermal solar power plant configuration that will be discussed later. All mirror configurations have in common that the mirrors must track the suns movement in the sky in order to maximize the concentration throughout the day. This can be done in either one or two axes. A system using one-axis tracking often have very large mirror assemblies and follows the suns natural path over the sky. Two-axis tracking is done with smaller mirror assemblies.

6.1.2 Thermal storage

Thermal storage capabilities are the key to cost efficient and more flexible concentrating solar power plant operation. With a thermal storage the plant owner is able to dispatch power when it's most valuable which often is in the evening when there is low or little incoming solar irradiation. There are a number of different types of solutions that is both in use and under development. The type of thermal storage that has gained the most attention in later years is molten nitrate that is used both as thermal media and as standalone thermal storage in systems with a different heat media in the solar concentration field. Other types of storage mediums are rock, sand and oil. [2]

6.1.3 Power cycle

Almost all currently operating solar trough and power tower systems uses a Rankine cycle to generate power. Water is heated up producing high pressure steam which is fed into a steam turbine coupled to a generator producing power. The steam is then condensed and returned to the boiler. What temperature and pressure used in the system depends on the steam turbine design and what is used to generate the steam. In concentrating solar plants applications the thermal heating fluid media is between 400 to 600 degrees Celsius. This means that steam around 350 to 550 degrees Celsius and 100 bar is common steam data.

Parabolic dish systems use a heat engine to produce power. The most common type of heat engine is a Stirling motor but experiments with the use of Brayton cycled engines have been conducted.

The most concentrating solar power plants are located in areas with little or no water because of the high amount of solar irradiation, large amount of sunny days and dry climate. This causes a problem when the vapor in the steam cycle should be condensed after leaving the turbine. Many plants use an air condenser, where the steam is cooled and condensed back to water with the surrounding air instead of the more common use of water as cooling medium. [3]

6.1.4 Thermal media

In thermal solar power plants operated today a variety of different thermal media is used. The thermal media is often mentioned as the thermal heating fluid or just “THF” which will be used in this report. Thermal media is referred to what kind of media that is used to transport heat from the concentrating apparatus to the power cycle. Some systems that use a heat engine don’t use any thermal heating fluid at all. The most common type of THF is thermal oil that can be heated up to around 400 degrees Celsius. There are also systems which uses steam throughout the system or a mixture of salt that is molten. Salts can be heated to around 500 degrees Celsius but needs an advance control system to prevent the molten salt to freeze which occur around 200 degrees Celsius. [4] [5]

6.2 TYPES OF CONCENTRATING SOLAR POWER PLANTS

In this section the most common types of concentrating solar power plant designs will be presented with a short description.

6.2.1 Parabolic trough

The sun's energy is concentrated by parabolically curved, trough-shaped reflectors onto a receiver pipe running along the inside of the curved surface. The medium pumped through the receiver pipes is heated up by the concentrated irradiation and then used to heat up water producing steam. The steam is then used to power a steam turbine coupled to a generator. The mirrors with absorber pipes are typically placed in parallel rows along a north to south axis to be aligned towards the sun as much as possible. A tracking system then angles the mirrors and pipes to minimize the incidence angle from the solar beams. Trough systems can incorporate thermal storage that enables the system to be operated in to the evening. Many currently operating trough systems are hybrid that means they are also support fired with an alternative fuel often being natural gas when the solar irradiation is not enough to run the plant. A typical parabolic trough concentrating solar power plant can produce between 50 MW up to 100 MW of electrical power. One of the largest now operating concentrating solar power plant, the Shams 1, is of parabolic trough type. Shams 1 have a power output of 100 MW and are located in the United Arab Emirates. [4] [5]

Figure 1 Parabolic trough collector. [6]

6.2.2 Power tower

Power tower systems use one central receiver mounted on top of a tower. A large amount of mirrors which are sun tracking in two axes, so called heliostats, is then concentrating the incoming solar irradiation on to the receiver. The heliostats are placed in front and around the tower and are laid out to maximize the performance of the power plant. In the receiver a thermal heating fluid is circulated which is being heated to a high temperature. The thermal heating fluid is then used to heat up water to steam that is used to power a steam turbine coupled with a generator producing electricity. Different kind of thermal heating fluids is used in power tower system ranging from air, oil and molten nitrate. In recent constructed power tower systems molten nitrate is used as thermal heating fluid. Molten nitrate is also the most common medium used in thermal heating storage that eliminates the need for a heat exchanger between the thermal heating fluid and the fluid used in the thermal storage. [7]

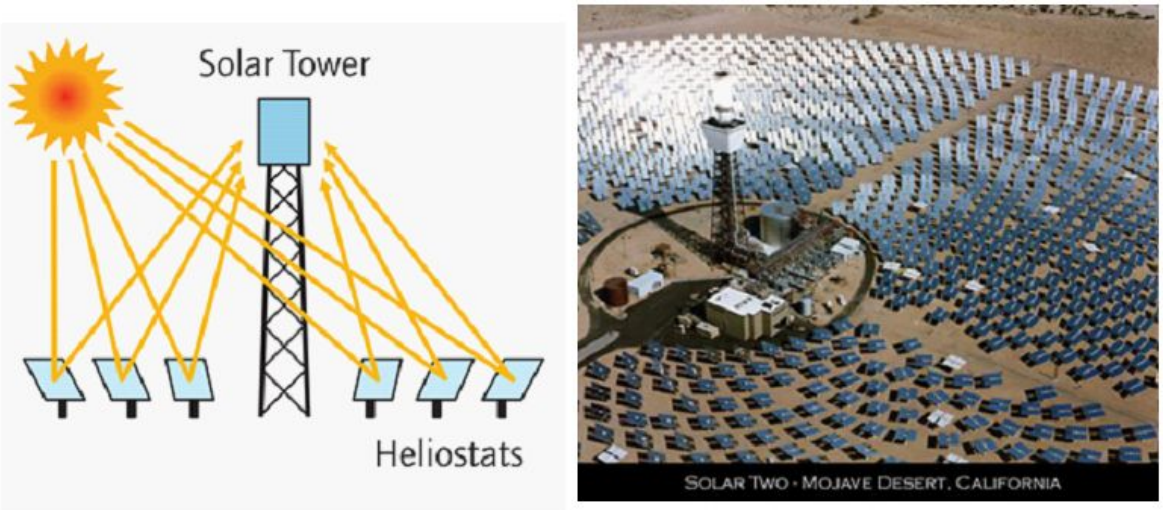

Figure 2 Power tower central receiver and heliostats. [6]

The power tower system is often very large and can produce as much as 200 MW of electricity. One of the largest concentrating solar power projects being developed right now is the Ivanpah project in the California Mojave desert in USA. Ivanpah consist of three power towers standing side by side and will be delivering 377 MW of electricity when it's finished. [8]

Figure 3 BrightSource Ivanpah central receiver and heliostat field under construction. [8]

6.2.3 Parabolic dish

The parabolic dish system utilizes a large parabolic mirror that follows the sun's movement in two axis in order to concentrate the incoming irradiation on a receiver in the mirror focal point. The receiver is fixed to the dish and is typically a heat powered motor meaning that the concentrated heat is used direct in the receiver to produce electricity. Stirling and Brayton cycle engines are the most commonly used types of heat engines in parabolic dish systems. The setup has been realized in plants producing up to 5 MW of electricity where each parabola with a heat engine produces up to 50 kW electricity with a peak efficiency of 30 percent net. [9]

Figure 4 Parabolic dish collector with heat engines. [6]

6.2.4 Linear Fresnel

The linear Fresnel system works in the exact same way as the parabolic trough system with the difference being in the collector and mirror design. The linear Fresnel system uses an elevated absorber with several mirrors mounted under the absorber tube. The mirrors are made of small strips that are slightly bended and focus the solar irradiation on to the overhead absorber tube. This means that the receiver tube and the mirrors are not mounted on the same tracking device giving the mirrors more flexibility to track the sun's movement over the sky to maximize the concentration of solar irradiation. The linear Fresnel system has a lower investment coast than a parabolic trough system at the same power output specification. It also has a lower maintenance and operation cost and uses less land space. The big disadvantage of the linear Fresnel is that it has a lower solar to electricity efficiency than the parabolic trough system. [10]

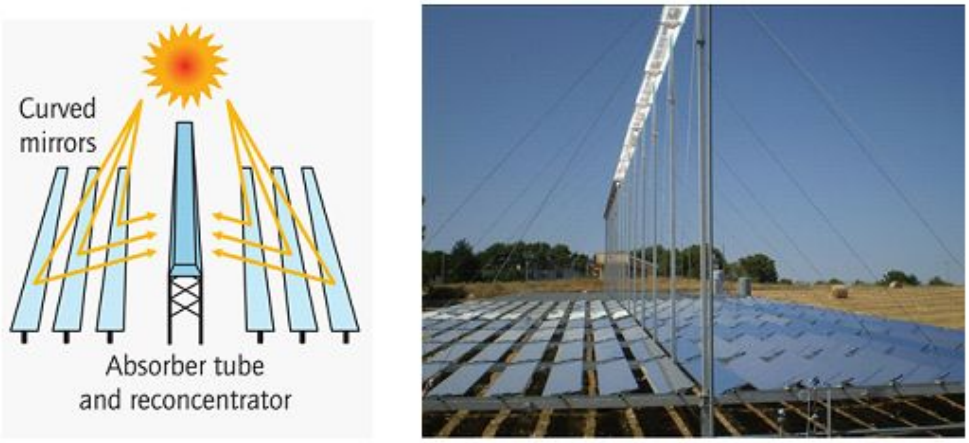

Figure 5 Linear Fresnel collector. [6]

6.3 AVAILABLE SOLAR IRRADIATION

The location of the thermal solar power plant is very important. The amount of incoming irradiation must be high and even during the day and throughout the year. The closer the plant is located to the equator the better. Most of the concentrating solar plants in Europe are located in the south of Spain. Some are also located in the south parts of Italy. In North America there is a concentration of plants in the southwest, in states like New Mexico, Nevada and southern California. [11] North Africa is also a suitable location for concentrating solar power plants but because of politically instable conditions not many plants are being built or operating there. [12]

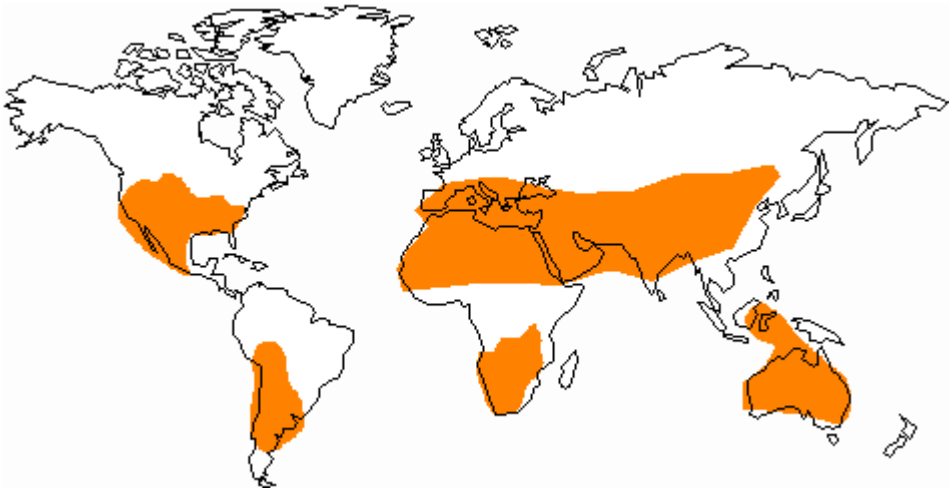

Figure 6 Orange marked area suitable for concentrating solar power. [13]

The marked areas in Figure 6 shows areas well suited for concentrating solar power because of high solar insolation. Concentrating solar power plants could be built outside of the marked areas but the collector field would have to be very large to compensate for the lower amount of solar insolation.

Exact calculations of the incoming solar irradiation will be conducted later on in the report.

6.4 Reference system

In this master thesis a base configuration of a concentrating solar plant will be chosen and modeled in the simulation tool Dymola. The most common and mature technology for thermal solar power is the parabolic trough design with indirect two-tank thermal storage capability. [11] Another system design that is becoming more and more developed and interesting for large size applications is the power tower solar power plant with a two tank direct thermal storage using molten nitrate throughout the system. [14] After revising the list of currently operating solar power plants the parabolic trough design with two-tank indirect thermal storage was chosen as the system to be built and simulated. In order to model the system correctly regarding incoming solar irradiation a specific location on earth for the power plant is also needed which will be discussed later on.

Because of the many different types of configuration and design of thermal solar power plants and the restricted amount of time given to conduct this master thesis a single configuration will be chosen. This system will serve as basic system when specific components and system design is developed.

In order to validate the concentrating solar power plant model built in Dymola a reference system is needed. It's rather tricky to find exact data from different now operating concentrating solar power plants. The plants are owned by private companies and incorporate a lot of unique company technology that is why specific design parameters and values of interest are kept secret. The National Renewable Energy Laboratory that serves under the department of energy in USA is listing a lot of data on different concentrating solar power plants. One of them is Andasol-I with sister plant Andasol-II located in south east of Spain. These power plants are of the same type as the basic system chosen earlier and relatively new. Because of the rather extensive information given about these plants it is chosen to serve as a reference system for this thesis. Plant data will be presented in Table 1 below.[15]

Plant name	Andasol-I and Andasol-II
Plant location	Aldeire y La Calahorra, Spain
Plant type	Parabolic trough
Start date	June 1, 2009
Receiver type	Schott PRT-70
Sun tracking	One axis in north-south direction
Collector type	Flabeg RP-3
Thermal heating fluid type	Dowtherm A
Turbine type	Siemens SST-700 50MW steam turbine
Thermal heating storage type	Two-tank indirect with molten solar salt

Table 1 Andasol-I and Andasol-II technical data

The thermal heating fluid used in Andasol-1 and Andasol-II are of the type Dowtherm A. The system being modeled will use another type of thermal heating fluid manufactured by Eastman with product name Therminol VP-1. Therminol is commonly used in a lot of now operating concentrating solar power plants. [16] The reason for this is that more technical data is available about the Therminol thermal fluid.

7 MODELLING THE SOLAR POWER PLANT

To model the chosen type of concentrating solar power plant the different components of the system described in section six must be implemented in Dymola. There are no solar power specific components present in the libraries available from Modelon today. To start with a very simple set of components will be made to get to know the software and Modelica better. Then a more detailed set of components will be developed.

After implementation the components will be evaluated against available data to make sure a correct implementation was made. When the different component models are working properly they will be connected together into a system model that will be validated against performance data given by the operator of the reference system.

7.1 MEDIA MODELS

Both the thermal heating fluid pumped through the receivers and the fluid used in the thermal heat storage needs to be implemented in Dymola. To implement a media model in Dymola a table of different thermodynamic properties is stated at a couple of predefined temperatures. The program then interpolates the exact value needed in the calculations. This means that different media properties like density, specific heat capacity and so on are implemented as linear functions.

The thermal heating fluid chosen for this thesis is Therminol VP-1 because of its documented use in many parabolic trough systems around the world and the availability of technical data provided by the manufacturer Eastman Chemical Company. Therminol is a clear transparent synthetic oil made of a eutectic mixture of 73.5 % diphenyl oxide and 26.5 % biphenyl. The oil has one of the highest thermal stabilities of all organic heat transfer fluids and is stable in liquid phase between 12 ℃ up to 400 ℃. This makes it ideal for use in concentrating solar power applications. [17]

The fluid used in the thermal heating storage is a mixture of 60 % $NaNO_3$ and 40 % KNO_3 by weight often referred to as solar salt. Solar salt is used because of its thermodynamic properties that are high heat capacity, high density, relatively low cost and low vapor pressure. The low vapor pressure makes the salt storage very easy because no pressurized salt tanks are needed. Another favorable feature of solar salt is the high temperature stability and liquid phase up to 560 degrees. The downside of solar salt is that is has a rather high freezing point and start to crystalize at 238 ℃ and is completely solid at 220 ℃. This means that special care must be taken to prevent the salt from freezing causing major damage to pipes, pumps and heat exchangers. [18]

The thermodynamic properties of solar salt were implemented in the same way as the thermal heating fluid. A linear table describing different properties at different temperatures is supplied and Dymola then uses linear interpolation to calculate the needed thermodynamic properties at the current state.

7.1.1 Properties of Therminol VP-1

Some key thermodynamic properties for Therminol VP-1 are listed in Table 2 below. [19]

Property	**Value**
Crystallizing Point	12 ℃
Autoignition Temperature (ASTM D-2155)	621 ℃
Kinematic Viscosity, at 100 ℃	0.99 cSt
Density at 25 ℃	1060 kg/m^3
Coefficient of Thermal Expansion at 200 ℃	0.000979/℃
Normal Boiling Point	257 ℃
Optimum use range, liquid phase	12-400 ℃

Table 2 Therminol VP-1 properties.

The thermodynamic properties supplied to Dymola is listed in Table 3 below

Property	**Range between 12** ℃ **and 427** ℃
Density $[kg/m^3]$	1071 to 651
Heat capacity $[kJ/kg \cdot K]$	1.52 to 2.77
Conductivity $[W/m \cdot K]$	0.1370 to 0.0695
Enthalpy $[kJ/kg]$	0.0 to 872.4

Table 3 Thermodynamic properties of Therminol VP-1.

The exact values for the listed properties are given by Eastman in the technical information folder for Therminol VP-1. [19]

After implementation of the Therminol VP-1 media model some of its thermodynamic properties were plotted to verify that the model behaves correctly.

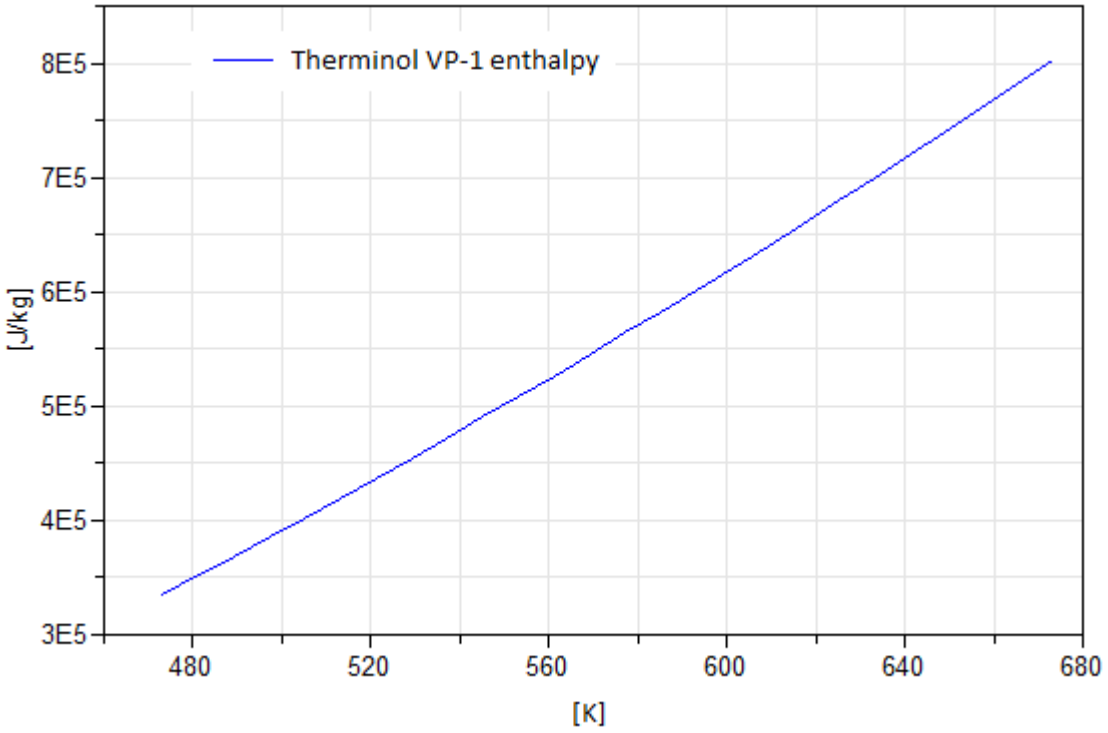

Figure 7 Therminol VP-1 enthalpy versus temperature plot.

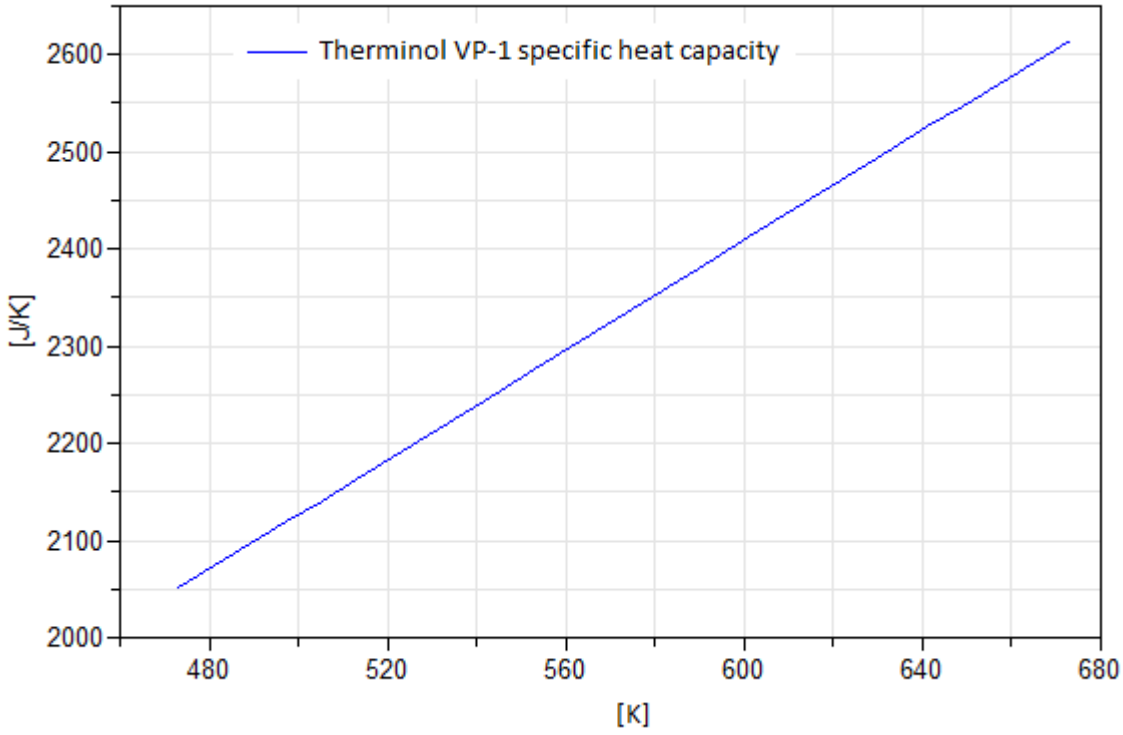

Figure 8 Therminol VP-1 specific heat capacity versus temperature plot.

From these graphs it's stated that the media model behaves as expected.

7.1.2 Properties of solar salt

The properties of solar salt are given by a set of temperature dependent relationships. Tables with the thermodynamic properties were created in Microsoft Excel and then copied to the media model in Dymola.

The following set of equations was used to create the solar salt media model. [20]

Density	$2090 - 0.636 \cdot (T - 273.15) \quad [kg/m^3]$ (1)
Heat capacity	$1443 + 0.172 \cdot (T - 273.15) \quad [J/kg \cdot K]$ (2)
Conductivity	$0.443 + 1.9 \cdot 10^{-4} \cdot (T - 273.15) \quad [W/m \cdot K]$ (3)
Viscosity	$\frac{22.714 - 0.12 \cdot (T - 273.15) + 2.281 \cdot 10^{-4} \cdot (T - 273.15)^2 - 1.474 \cdot 10^{-7} \cdot (T - 273.15)^3}{1000} \quad [Pa \cdot s]$ (4)
Isobaric expansion coefficient, beta	$\frac{0.636}{2263.72 - 0.636 \cdot T} \quad [K^{-1}]$ (5)
Isothermal compression coefficient, kappa	$10^{-11} \cdot e^{\left(1.37 \cdot 10^{-3} \cdot (T - 273.15)\right)} \quad [Pa^{-1}]$ (6)
Enthalpy	$0.086 \cdot T^2 + 1396.0182 \cdot T \quad [J/kg]$ (7)
Entropy	$1396.0182 \cdot ln(T) + 0.172 \cdot T \quad [J/kg \cdot K]$ (8)

A correlation of specific volume versus pressure is not available for solar salt and therefor it's not possible to obtain a value of the isothermal compression coefficient, kappa. The coefficient is very small for solar salt in liquid phase, in the order of $10^{-10}\ Pa^{-1}$. With this in mind the value of the isothermal compression coefficient for mercury that is also very small was used as an approximation for the kappa value of solar salt.

After implementation of the solar salt media model the same test cases as for the Therminol media models were conducted.

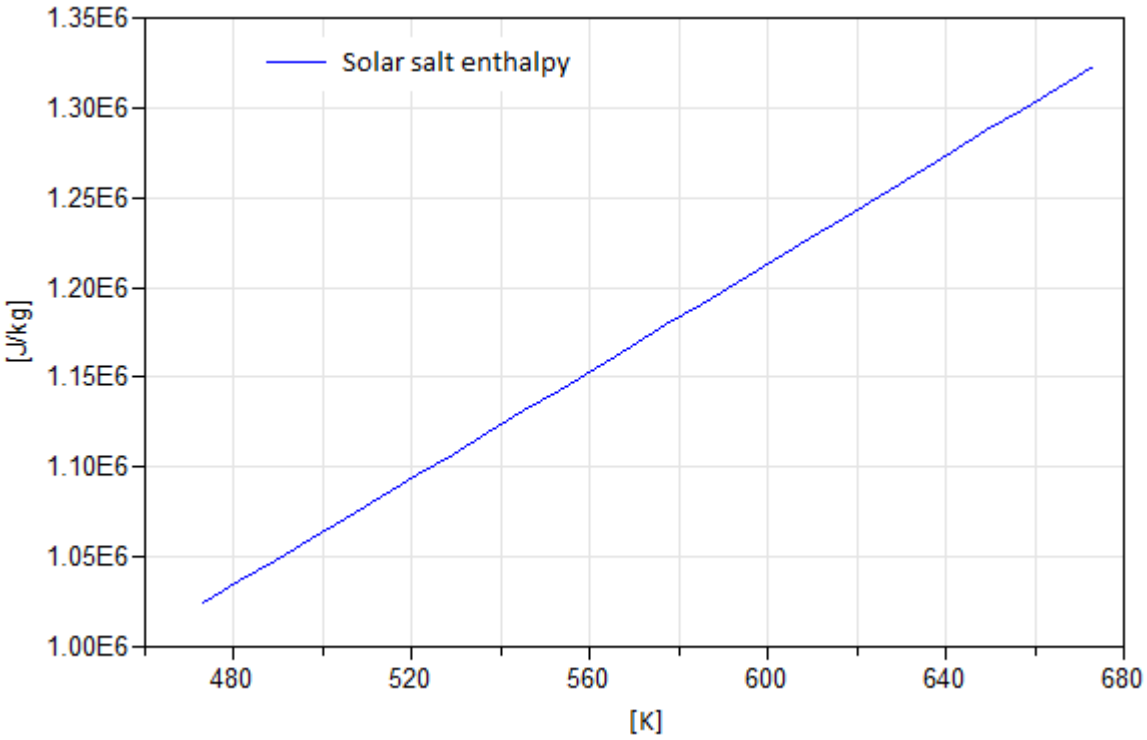

Figure 9 Solar salt enthalpy versus temperature plot.

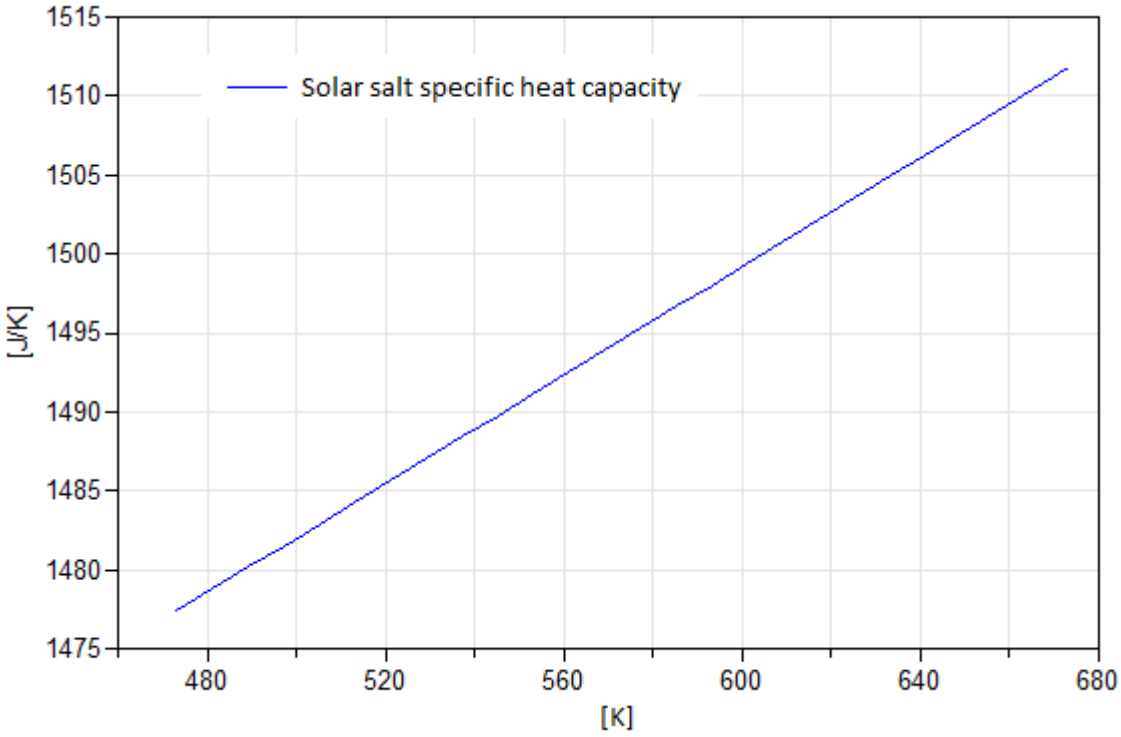

Figure 10 Solar salt specific heat capacity versus temperature plot.

From these graphs it's stated that the solar salt media models works as expected.

7.2 SIMPLE SYSTEM MODEL IN DYMOLA

A simple yet practice related model of a concentrating solar power plant was made to get a picture of how the system is supposed to work and give a hint of problems and difficult steps in the modeling process. By doing a simple version a lot of knowledge in the software suit is gained leading to faster development time when a more advance version is to be made. The tradeoffs for the simple system consist of using just a ramp to simulate reflected solar irradiation on to the receiver, an absorber pipe with constant heat transfer properties with zero losses and a very simplified Rankine cycle. An evaluation of the simple system is then made to identify possible problems for a more detailed system model. The different parts of the model are discusses below.

7.2.1 Incoming solar irradiation

For the simple system a ramp function is used to simulate the rising amount of incoming solar irradiation throughout the day. This ramp is placed inside the collector model. The ramp starts from zero and stops at $60 \cdot 10^6$ with a duration of 8000 seconds. This is the total amount of heat being concentrated onto the receiver. No tracking function is implemented for the collector to minimize the incidence angle between the beam and the collector aperture normal.

7.2.2 Concentrating device

The parabolic trough concentrator consists of two major parts, the reflective parabolic shield called collector and the heat absorbing tube called the receiver. The collector's job is to reflect as much incoming solar irradiation onto the receiver as possible while the receiver's task is to transfer as much of the reflected heat to the heat transfer media.

In this first simple model a pipe whit constant heat transfer properties is used as receiver. Reflected solar irradiation is simulated with a ramp function to emulate a sunrise.

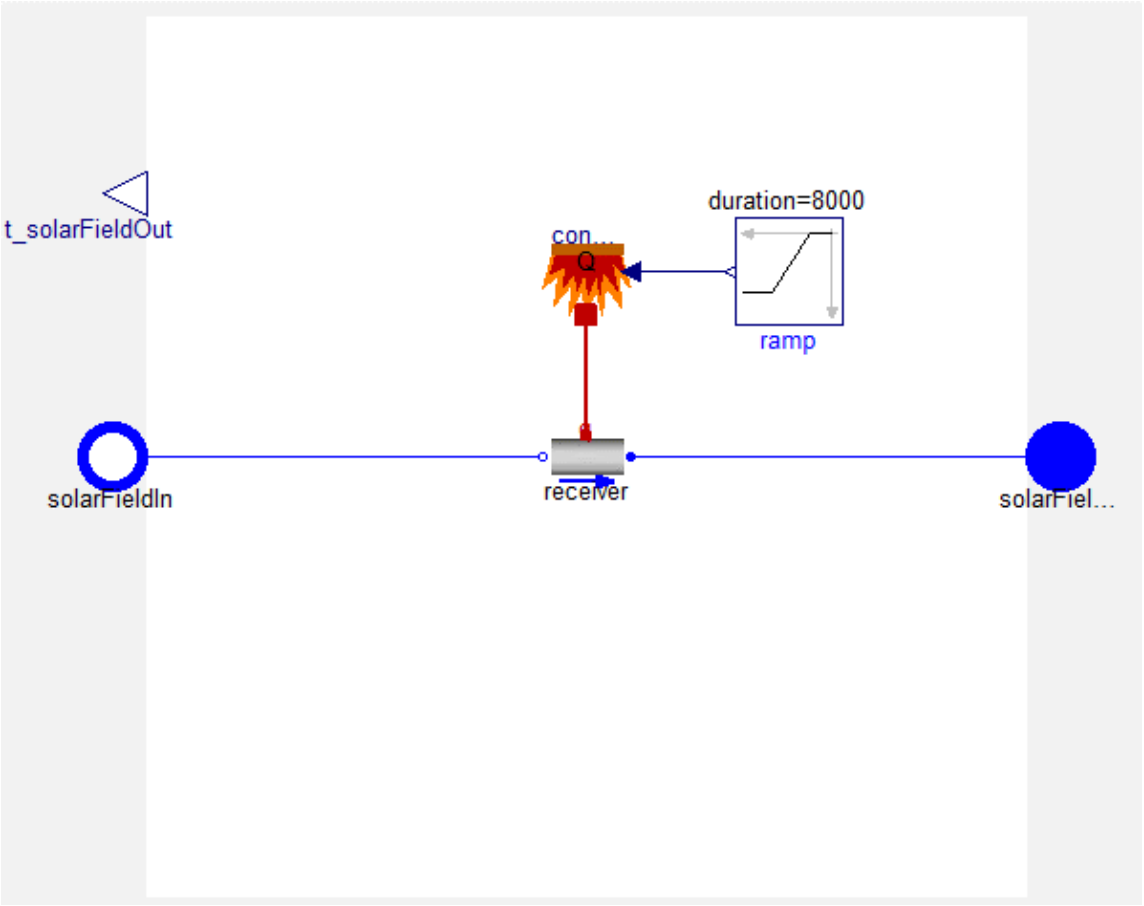

Figure 11 Overview of the simple solar collector model in Dymola.

The pipe has a lenght of 89856 meter which is the total solar loop length for Andasol-II and a diameter of 0.07 meter which is the diameter of the absorber tubes used. The heat transfer area is approximated to half of the pipe outer area and the heat transfer coefficient is approximated to 15 W/m^2K.

7.2.3 Thermal storage

The basic principle of the thermal heat storage is to heat the thermal storage medium with the help of the THF when the solar field is absorbing more than a certain amount of heat needed to power the Rankine cycle. The process is then reversed to heat the THF when the solar field is absorbing less than a certain value or nothing. The system consist of two large, well-insulated tanks with ambient pressure, two pumps to pump the molten salt from one tank to the other and vice versa, a heat exchanger to transfer heat from the molten salt to the THF and vice versa and valves to control the flow.

To make the system work this way a vast amount of automatic control is needed to control valves and pumps to keep the right temperatures, flow rates and tank levels. Unfortunately not much information is supplied about how these systems are designed in detail in existing concentrating solar power plants.

There will be a loss in the heat exchanger between the thermal oil and the solar salt. That means that the heated solar salt will reach a temperature below the maximum thermal oil temperature of 393 ℃. If the heat exchanger has a pinch point design of 10 ℃ the heated solar salt will reach a

temperature of 383 °C. When the system is reversed and the thermal oil is heated by the solar salt the thermal oil outlet temperature from the heat storage will be 373 °C. This will affect the performance of the steam generating process that usually is optimized for the desired thermal heating fluid temperature of 393 °C.

In this simplified system no actual thermal storage will be implemented. Instead a bypass module is implemented which bypass the thermal heating fluid back to the collector field when the thermal fluid outlet temperature is below the desired temperature of 393 °C. This makes the thermal fluid recirculate through the collector field until right temperature is reached.

7.2.4 Power cycle

The Rankine cycle consists of a forced circulation drum boiler. There is no steam turbine after the drum boiler at this point and the produced steam is dumped in a sink. Heat is supplied from the thermal heating fluid to the drum boiler via a heat exchanger.

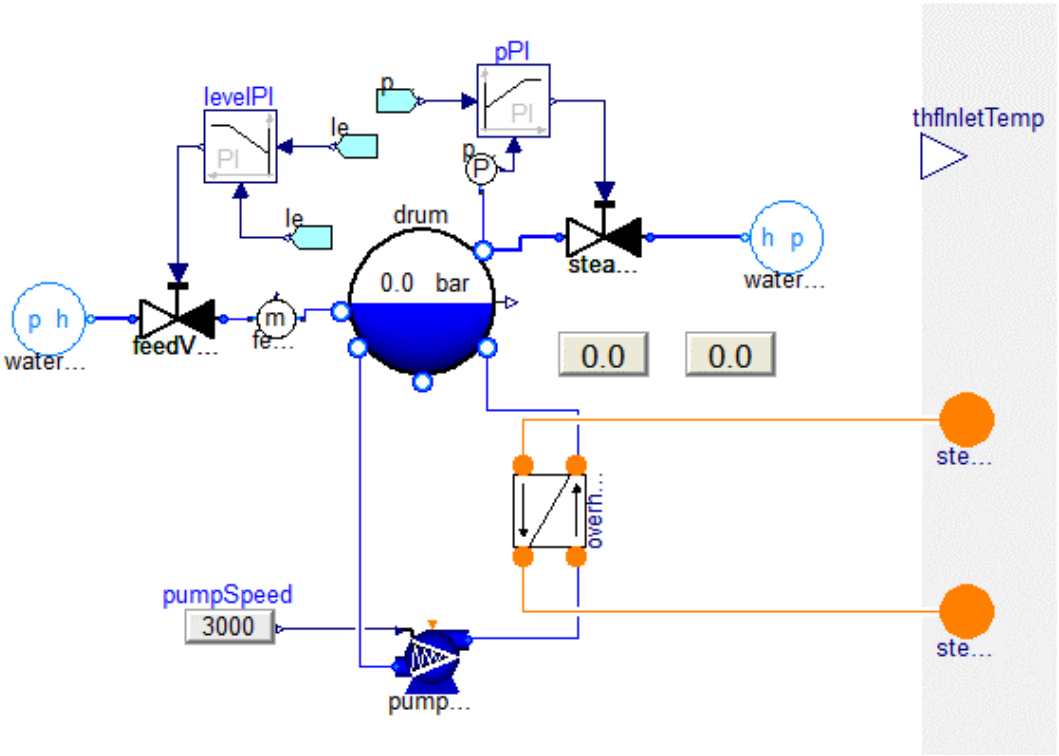

Figure 12 Overview of the Rankine cycle model for the simple system in Dymola.

7.2.5 Control

There are two control units, *bypassControl* and *pumpControl*. The bypass control unit makes sure that the thermal heating fluid has the correct temperature before entering the Rankine cycle. If the temperature is to low the thermal fluid is re-circulated in the collector loop until right temperature has been reached.

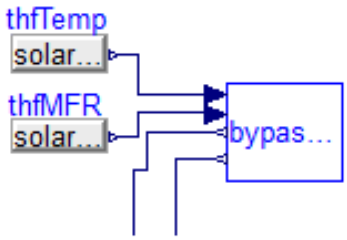

Figure 13 The bypass control unit used in the simple system.

The inputs shown in Figure 13 are the mass flow rate and the outlet temperature of the thermal fluid from the collector field. The two outputs goes to the valves setting the valve opening to redirect the thermal fluid. The mass flow rate was just used in testing and has no real purpose in controlling the bypass of thermal fluid from the Rankine cycle.

The pump control consists of a PI-regulator that regulates the mass flow rate of the thermal fluid to keep the outlet temperature at a set point temperature of 393 ℃.

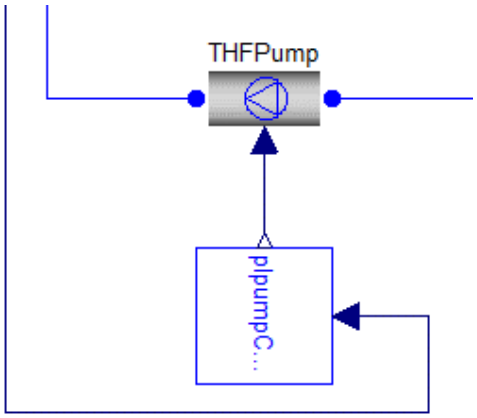

Figure 14 The control unit for the thermal fluid pump connected to the pump in the simple system.

The inputs to the pump control block are the thermal heating fluid outlet temperature form the collector field used as measuring signal for the PI regulator.

7.2.6 Evaluation of the simple system

The results from the simple system and further research in the topic shows that a much more detailed model for the collector is needed. The majority of the losses in the system will occur in the collector field because of its very long length, up to 90000 meter. The losses will be heat losses in the receiver by radiation and convection to the surroundings and in the collector due to imperfections in the mirror and the fact that the incidence angle will vary during the day. These losses will have to be modeled in the more detailed model in order to get more accurate results. The collector will also have tracking capabilities in order to minimize the solar irradiation incidence angle.

There is no real way to model the suns movement and irradiation to earth that differs throughout the day in the simple system that is needed in the more detailed model. A separate sun model will be made were user supplied values of direct normal irradiation will be used to calculate the correct irradiation at the current time for the actual model location on earth.

In the simple system no thermal heat storage was modeled. In the detailed system a heat storage has to be implemented. This rapidly increases the complexity of the control system that has to know when the system should charge the thermal heat storage, discharge heat from the heat storage and dump heat when the storage is full. Dumping is done by intentionally defocus a part of the collector field and thereby absorbing less heat to the thermal oil.

With these improvements in mind a decision was made to not continue the development of the Rankine cycle. The detailed system will only be using a highly simplified model of the Rankine cycle.

7.3 Detailed system model in Dymola

In order to simulate the concentrated solar power plant model with higher accuracy a more detailed system model is needed compared to the simple system. This primarily consists of heat loss models for the collector system and a more detailed calculation of how much solar irradiation that can be absorbed. There is some form of heat loss in almost all components of the system but most of them occur in the solar collector assemblies. The reason for this is that the solar collector field is very large in terms of length. In the Andasol case the total absorber tube length is over 80000 meters. Other pipes within the system are assumed to be well insulated. For obvious reasons there is no insulation on the absorber tubes. Regarding calculations of incoming solar irradiation there is also a need to use real measurements of solar irradiation and use them in the model. The measurements of solar irradiation for the specific location are parsed to the model from a CSV file supplied by the user.

To bring some clarity in how the procedure looks like a simple calculation roadmap from incoming solar irradiation to net electric output is shown in Figure 15.

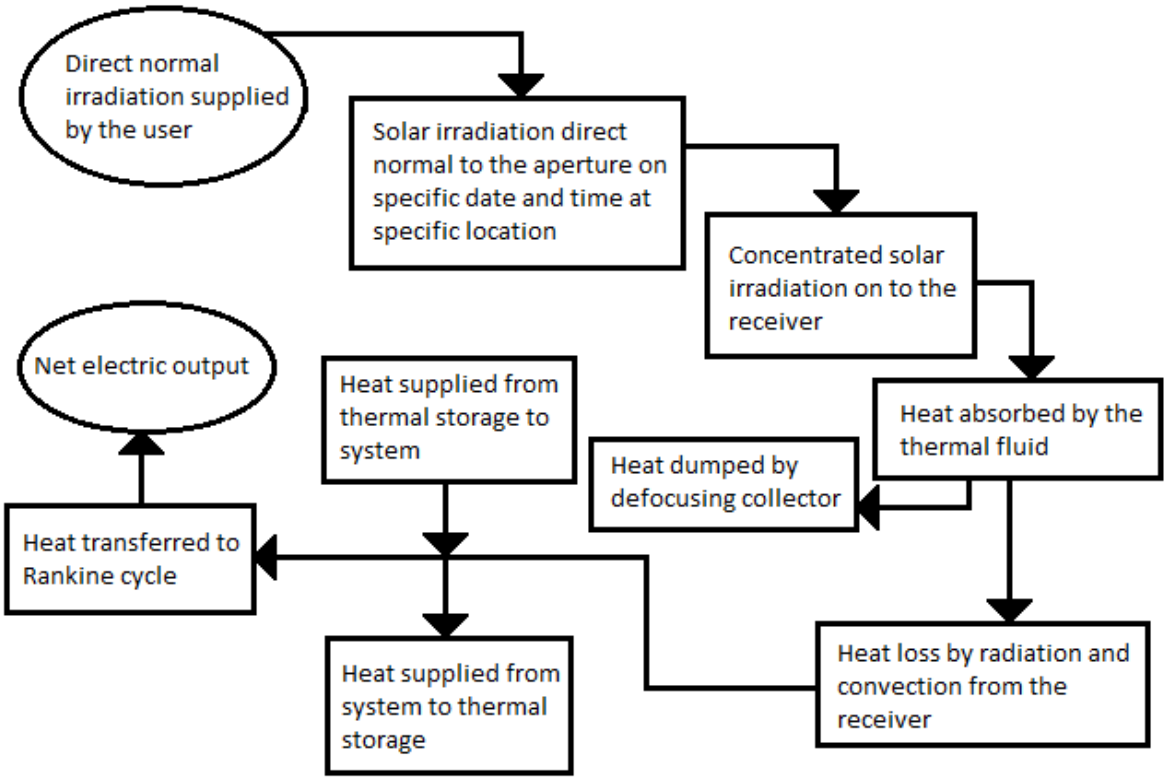

Figure 15 Calculation roadmap for the detailed system in Dymola.

7.3.1 Incoming solar irradiation

The incoming solar irradiation from the sun can be divided between beam radiation and diffuse radiation. Beam radiation is the solar radiation received from the sun without having been scattered by the atmosphere and is referred to as direct solar radiation. Diffuse solar irradiation is solar radiation received after being scattered by the atmosphere and changed direction.

In concentrating solar power systems calculations are only made with direct solar radiation. This is because the incidence angle of the diffuse solar radiation on earth is impossible to predict and it's therefor hard to design a collector assembly to concentrate this radiation. Any diffuse solar radiation that hits the collector and can be concentrated onto the receiver is just considered as a bonus. [21]

The solar data is supplied by the user in a CSV file with hourly values of direct normal insolation in the sun model.

7.3.1.1 Sun model

To calculate the direct solar radiation onto a surface, in this case a solar collector assembly, for a specific date, time and location on earth a set of different equations is needed.

When calculating the angles that are needed to determine how much direct beam radiation will hit the collector, solar time is used which differs from the local time on earth. The difference in minutes can be expressed as following: [21]

Solar time - local time = $4 \cdot (L_{st} - L_{loc}) + E$ (9)

Where L_{st} is the standard meridian for the local time zone, L_{loc} is the longitude of the location in degrees west and E is the equation of time.

Equation of time is expressed as:

$$E = 229.2 \cdot (0.000075 + 0.001868 \cdot \cos B - 0.032077 \cdot \sin B - 0.014615 \cdot \cos 2B - 0.04089 \cdot \sin 2B) \quad (10)$$

Where

$$B = (n - 1) \cdot \frac{360}{365} \quad (11)$$

And n = day of the year.

The angle of incidence of direct solar radiation onto a north to south axis tracking collector which is used at the Andasol plant can be calculated as following: [21]

$$\cos\theta = (\cos\theta_z{}^2 + \cos\delta^2 \cdot \sin\omega^2)^{\frac{1}{2}} \quad (12)$$

Were

δ is the declination, the angular position of the sun at solar noon. [21]

$$\delta = 23.45 \cdot \sin\left(360\frac{284 + n}{365}\right) \quad (13)$$

ω is the hour angle, the angular displacement of the sun east or west of the local meridian due to rotation of the earth on its axis at 15° per hour. [22]

$$\omega = (t_{sol} - 12) \cdot 15 \quad (14)$$

θ_z is the zenith angle, the angle of incidence of beam radiation on a horizontal surface. [21]

$$\theta_z = \cos\phi \cdot \cos\delta \cdot \cos\omega + \sin\phi \cdot \sin\delta \qquad (15)$$

Were ϕ is the latitude.

The incidence angle is the angular difference θ between the normal to the aperture and the actual solar irradiation that can be seen in Figure 16. When the direct beam radiation is not normal to the plane of the collector aperture there is a loss of direct beam radiation that scale with the cosines of the angle θ.

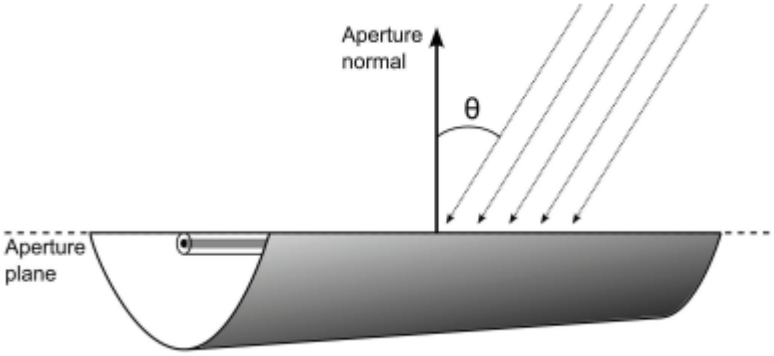

Figure 16 A graphical interpretation of the angle between the aperture normal and the solar irradiation. [21]

The total radiation incidence per square meter on to the collector field is equal to the specific direct normal irradiation scaled with the cosine of the incidence angle

$$I_{field} = I_{bn} \cdot \cos\theta \qquad [W/m^2] \qquad (16)$$

The sun model output is the effective solar irradiation per square meter for the aligned collector. This means that the calculations for collector tracking have been implemented in the sun model and not in the collector model.

7.3.2 Concentrating device

The concentrating device main task is to concentrate incoming solar radiation via a mirror called collector onto an absorber pipe called receiver. In the receiver a heat transfer fluid is pumped to absorb heat and transfer it to the steam generating system.

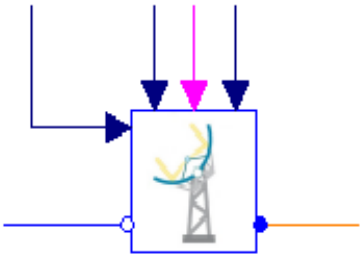

Figure 17 Overview of the solar collector for the detailed system in Dymola.

7.3.2.1 Collector

The collector is a mirror shaped as a cylindrical parabolic reflector focusing the incoming solar irradiation onto the absorber pipe. There are numerous equations to describe the geometry of the mirror and the image, distribution of solar radiation flux across the focus, it produces. It is assumed that the collector design already have been optimized which gives the parameters that should be

provided to the collector model in Dymola. The parameters of interest are the optical efficiency and collector aperture width and length.

The aperture width is the trough width and the total aperture area is the length of the collector times the aperture width. The total aperture area gives the total amount of solar irradiation that can be concentrated onto the receiver.

There are several loss models for the mirror that have to be taken into account. In this model a single parameter called optical efficiency, η_{opt}, is introduced to describe the total mirror efficiency. The different losses included in this parameter are listed in Table 4 below: [22]

Tracking error	Inability of the collector to perfectly orient along the tracking angle. Twisting of the collector about the lengthwise axis.	η_{track}
Geometry defects	Poor alignment of the mirror modules.	η_{geo}
Mirror soiling	Dirt or soiling on the reflective surface that decreases the reflected amount of solar irradiation onto the absorber pipe.	η_{soil}
General error	Any other loss not covered by previous categories.	η_{gen}

Table 4 List of different losses in the mirror.

This gives the optical efficiency:

$$\eta_{opt} = \eta_{track} \cdot \eta_{geo} \cdot \eta_{soil} \cdot \eta_{gen} \qquad (17)$$

This efficiency term is multiplied with the total radiation incidence on the collector calculated earlier in the sun model and the total aperture area and then gives the amount of incoming, reflected solar irradiation onto the receiver. The amount of incoming reflected solar irradiation is then used in the receiver model to calculate the amount of heat absorbed to the thermal heating fluid and the amount lost due to radiation and convection to the surroundings.

$$Q_{receiver} = I_{field} \cdot A_{tot,aperture} \cdot \eta_{opt} \quad [W] \qquad (18)$$

7.3.2.2 Receiver

In order to get more valid results from the receiver a more complex model is needed compared to the receiver model made in the simple model. This model has to account for various heat losses that occur along the receiver. These losses consist of radiation and convection, either natural in case in no wind or forced in case of wind, heat transfer from the outer glass casing of the receiver. Because of the long receiver length, in the Andasol case almost 90000 m, the temperature and heat losses will vary along the absorber axis. In this case the model is discretized which is done by dividing the absorber pipe in n number of segments. The heat transfer equations are then solved in each segment

and the total heat transfer for the whole receiver is the sum of the heat transfer in each element. This gives a much more accurate results as discussed in several studies in the subject. [23]

The receiver can be represented as a thermal resistant network as shown in Figure 19. The measurements and temperatures denoted in the equations that follows are marked in Figure 18 and Figure 19.

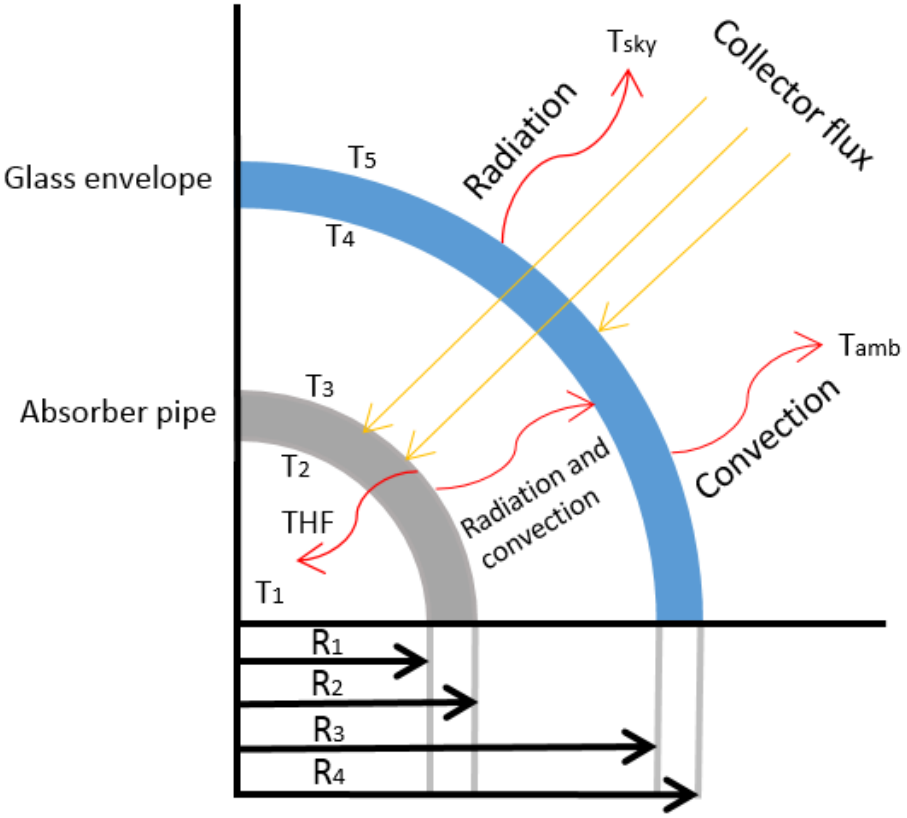

Figure 18 Measurements and heat flow in receiver.

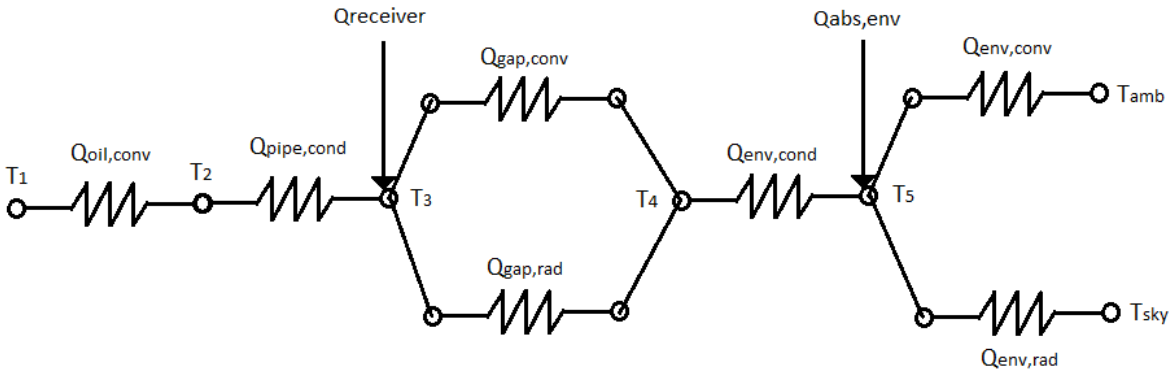

Figure 19 Receiver model represented as a thermal resistance network.

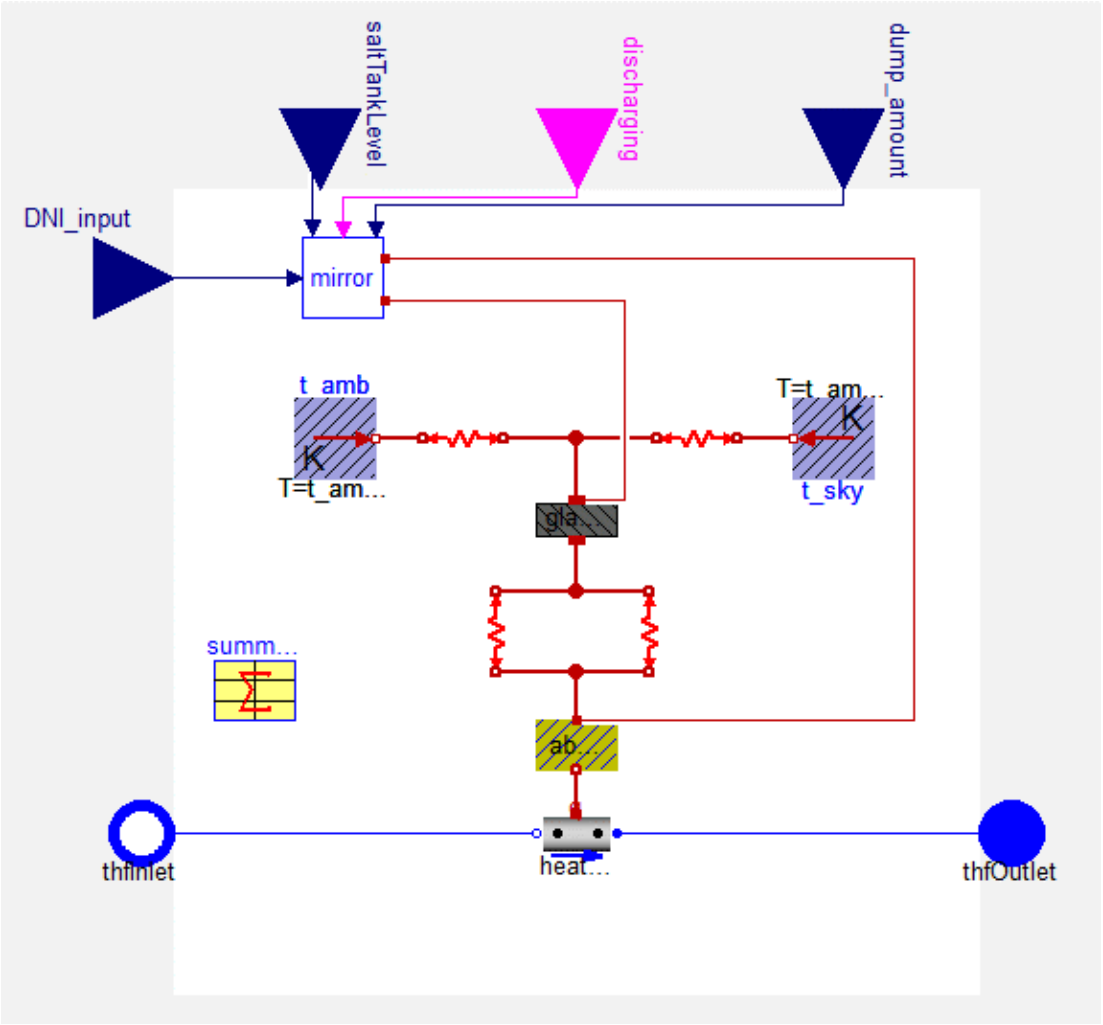

Figure 20 Overview of the collector model for the detailed system in Dymola with mirror and receiver.

The absorbed energy in the steel pipe that the THF is pumped trough is modeled with a standard conduction heat transfer model for a metal wall already developed by Modelon. It's assumed that the steel pipe is made out of standard carbon steel.

The heat transferred through the metal wall is then absorbed by the THF by convection in a pipe model also already developed by Modelon. The steel surface in commercial absorbers is coated with special materials to decrease radiation from the steel pipe surface. In the parameter settings for the receiver the surface emissivity of the steel pipe can be set to match values representing the current coating material.

From the steel pipe surface both convection and radiation occurs in the vacuum gap between the outer glass casing and the steel pipe. The convection is modeled with a standard convective heat transfer model developed by Modelon. When the gap between the steel pipe and the glass cover is under vacuum the convective heat transfer mechanism is molecular conduction between molecules. If the vacuum is lost by example a crack in the glass cover the heat transfer mechanism is free convection. [24] It is assumed that vacuum is always present in the gap for this model. The heat transfer coefficient for the vacuum of air is $k_{c,gap} = 0.0001115\, W/m^2K$. [23] The heat transfer coefficient is provided as a parameter for the user to change which means that simulations with different vacuum properties or vacuum with different gases than air can be made.

$$\dot{Q}_{gap,conv} = k_{c,gap} \cdot D_3 \cdot \pi \cdot L_{rec} \cdot (T_3 - T_4) \qquad (19)$$

There were no model for radiation present in the Dymola model library which had to be developed and can be expressed as following:

$$\dot{Q}_{gap,rad} = \pi \cdot D_3 \cdot L_{rec} \cdot \gamma_{gap,rad} \cdot (T_3 - T_4) \qquad (20)$$

$$\gamma_{gap,rad} = \sigma \cdot \left({T_3}^2 - {T_4}^2\right) \cdot \frac{T_3 + T_4}{\frac{1}{\varepsilon_3} + \frac{D_3}{D_4} \cdot \left(\frac{1}{\varepsilon_4} - 1\right)} \qquad (21)$$

Several assumptions are made in deriving this equation: nonparticipating gas in annulus, gray surfaces and long concentric isothermal cylinders. The glass is also assumed to be opaque to infrared radiation. These assumptions are not completely accurate but the errors caused are relatively small. [23]

The glass casing consists of a heat transfer model through a wall material with constant parameters developed by Modelon. The user needs to supply material data for the glass material such as density, specific heat capacity and thermal conductivity. Most receiver glass envelopes are made out of borosilicate glass that has a very low coefficient of thermal expansion. This makes them resistant to thermal shocks that are a very good property in concentrating solar power applications. The parameters that have to be specified in the model are listed in Table 5 below with corresponding standard values for borosilicate glass that is also used in Dymola for this model. [25]

Material property	Value for standard borosilicate glass
Density	$2300\ kg/m^3$
Specific heat capacity	$830\ J/kg \cdot K$
Thermal conductivity	$1.2\ W/m \cdot K$

Table 5 Material properties for borosilicate glass.

Most of the solar irradiation concentrated onto the receiver is absorbed as heat to the thermal heating fluid but the receiver glass cover also absorbs some heat. This raises the glass surface temperature and therefor creating a higher difference between the ambient temperature and the glass cover surface temperature. A higher difference in temperature means a higher rate of heat flow. The amount of heat absorbed by the glass can be expressed as following: [26]

$$\dot{Q}_{env,abs} = \dot{Q}_{receiver} \cdot \frac{\alpha_{env}}{\tau_{env} \cdot \alpha_{abs}} \qquad (22)$$

Some of the heat transferred through the glass casing is then lost by radiation due to temperature differences between the glass and the sky. Convective heat transfer also occurs and is either natural or forced depending if there is wind or not. Both the radiation and the convection models consist of a set of specific equations.

The radiation can be expressed as following when assuming the glass envelope to be a small convex gray body surrounded by a large black body which represent the sky: [23]

$$\dot{Q}_{env,rad} = \sigma \cdot \pi \cdot D_4 \cdot L_{rec} \cdot \left({T_5}^4 - {T_{sky}}^4\right) \qquad (23)$$

The sky temperature can be assumed to be 8 degrees lower than the ambient temperature. [22]

The convection from the outer surface of the glass envelope can be expressed as following:

$$\dot{Q}_{env.conv} = h_{amb} \cdot \pi \cdot D_4 \cdot L_{rec} \cdot (T_5 - T_{amb}) \qquad (24)$$

Where h_{amb} is the convective heat transfer coefficient to the ambient. The heat transfer coefficient varies depending on if it's wind blowing on the envelope or not. In no wind case there is natural convection and the heat transfer function can be expressed as following: [23]

$$h_{amb,nowind} = \overline{Nu} \cdot \frac{k_{56}}{D_4} \qquad (25)$$

Where the Nusselt number can be calculated using a correlation developed by Churchill and Chu for a long isothermal horizontal cylinder: [23]

$$\overline{Nu} = \left[\frac{0.60 + 0.387 \cdot {Ra_{D4}}^{0.1667}}{\left(1 + \left(\frac{0.559}{Pr_{56}}\right)^{0.5625}\right)^{0.2963}} \right]^2 \qquad (26)$$

$$Pr_{56} = \frac{\mu_{56} \cdot Cp_{56}}{\kappa_{56}} \qquad (27)$$

$$Ra_{56} = \frac{g \cdot \beta_{56}}{\frac{\kappa_{56}}{Cp_{56} \cdot \rho_{56}} \cdot \frac{\mu_{56}}{\rho_{56}}} \cdot (T_5 - T_{amb}) \cdot {D_4}^3 \qquad (28)$$

All thermodynamic properties are calculated at the mean temperature between the envelope surface temperature and the ambient temperature $T_{56} = \frac{T_5 + T_{amb}}{2}$

If there is wind, forced convection will occur and in this case the heat transfer function will be calculated in the same way as in the no wind case but the Nusselt number will instead be estimated with Zhukauskas' correlation for external forced convection flow normal to an isothermal cylinder as following: [23]

$$\overline{Nu} = C \cdot {Re_{D4}}^m \cdot {Pr_6}^n \cdot \left(\frac{Pr_6}{Pr_5}\right)^{0.25} \qquad (29)$$

$$Re_{D4} = w \cdot D_4 \cdot \frac{\rho_6}{\mu_6} \qquad (30)$$

$$Pr_5 = \frac{\mu_5 \cdot Cp_5}{\kappa_5} \qquad (31)$$

$$Pr_6 = \frac{\mu_6 \cdot Cp_6}{\kappa_6} \qquad (32)$$

The coefficients m, n and C are selected according to the Prandtl number and the Reynolds number as shown in Table 6 and Table 7. [22]

Reynolds number range	C	m
$0 \leq Re_{D4} < 40$	0.75	0.4
$40 \leq Re_{D4} < 1000$	0.51	0.5

$1000 \leq Re_{D4} < 2 \cdot 10^5$	0.26	0.6
$2 \cdot 10^5 \leq Re_{D4} < 10^6$	0.076	0.7

Table 6 Selection of coefficients C and m for the Nusselt depending on Reynolds number.

Prandtl number range	n
$Pr_6 \leq 10$	0.37
$Pr_6 > 10$	0.36

Table 7 Selection of coefficient n for the Nusselt number depending on the Prandtl number.

When the heat loss by radiation and convection from the envelope is known, and thereby the radiation and convection in the vacuum gap, the amount of heat absorbed by the thermal heating fluid is known:

$$\dot{Q}_{oil,conv} = \dot{Q}_{absorber} - \dot{Q}_{gap,rad} - \dot{Q}_{gap,conv} \quad (33)$$

$$\dot{Q}_{gap,rad} + \dot{Q}_{gap,conv} = \dot{Q}_{env,rad} + \dot{Q}_{env,conv} - \dot{Q}_{env,abs} \quad (34)$$

7.3.3 Thermal storage

The thermal storage task is to supply extra heat to the system when the solar irradiation is not enough or none. When the incoming solar irradiation is below a certain value the outlet temperature cannot reach the desired level of 393 ℃. This is when the thermal storage is used instead; heating the thermal heating fluid to 373 ℃. It's not possible to reach the design point temperature of 393 ℃ because of losses in the heat exchanger between the thermal oil and the salt.

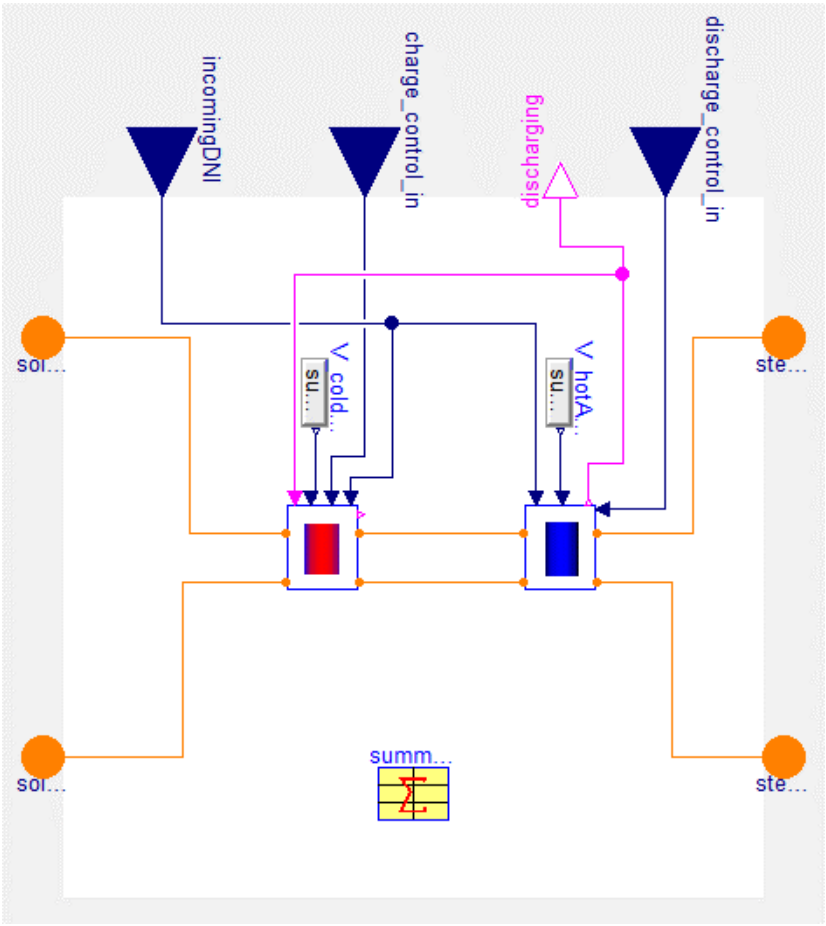

Figure 21 Overview of the thermal storage model for the detailed system in Dymola. The red icon represent the hot salt tank and the blue the cold salt tank.

The collector field for the Andasol power plant is over-dimensioned in order to be able to produce heat for both charging the thermal storage and the power cycle during the hours of the day with most solar irradiation. If no thermal storage was to be fitted to the system the collector field size could be reduced with approximately 40 %. After a couple of hours when the thermal storage is completely charged too much heat is absorbed just for the power cycle and a part of the collector field is intentionally defocused. [27]

The heat storage consists of a molten nitrate mixture and is heated up when the collector field absorbs more heat than necessary for the power cycle. The heat is transferred to the solar salt via a heat exchanger with a 10 ℃ pinch point making the salt 10 degrees cooler then the inlet temperature of the thermal heating fluid. When the solar salt is used to heat up the thermal heating fluid the system is reversed and the thermal fluid is heated up via the same heat exchanger. The thermal heating fluid will then reach an outlet temperature 10 ℃ below the solar salt inlet temperature.

It's assumed that the thermal storage tanks are well insulated and no loss model is implemented in the thermal storage model.

7.3.3.1 Charging the thermal storage

The charging of the solar salt is made by tapping off a part of the heated thermal fluid from the collector field and redirecting this to the heat exchanger between the thermal oil and the solar salt.

The mass flow rate of hot thermal fluid through the heat exchanger is determined with a simple formula and the fact that the minimum mass flow rate to the power cycle in known.

$$\dot{m}_{THF,main} = \frac{\frac{Q_{turbine}}{\eta_{powercycle}}}{h_{THF@393℃} - h_{THF@293℃}} = \frac{\frac{50 \cdot 10^6}{0.388}}{783100 - 539200} = 528.4\, kg/s$$

Any mass flow over this value is redirected to the heat exchanger in the thermal storage unit. The maximum mass flow rate of the thermal fluid pump is set to 1200 kg/s which gives a maximum mass flow rate of 671 kg/s to the thermal storage.

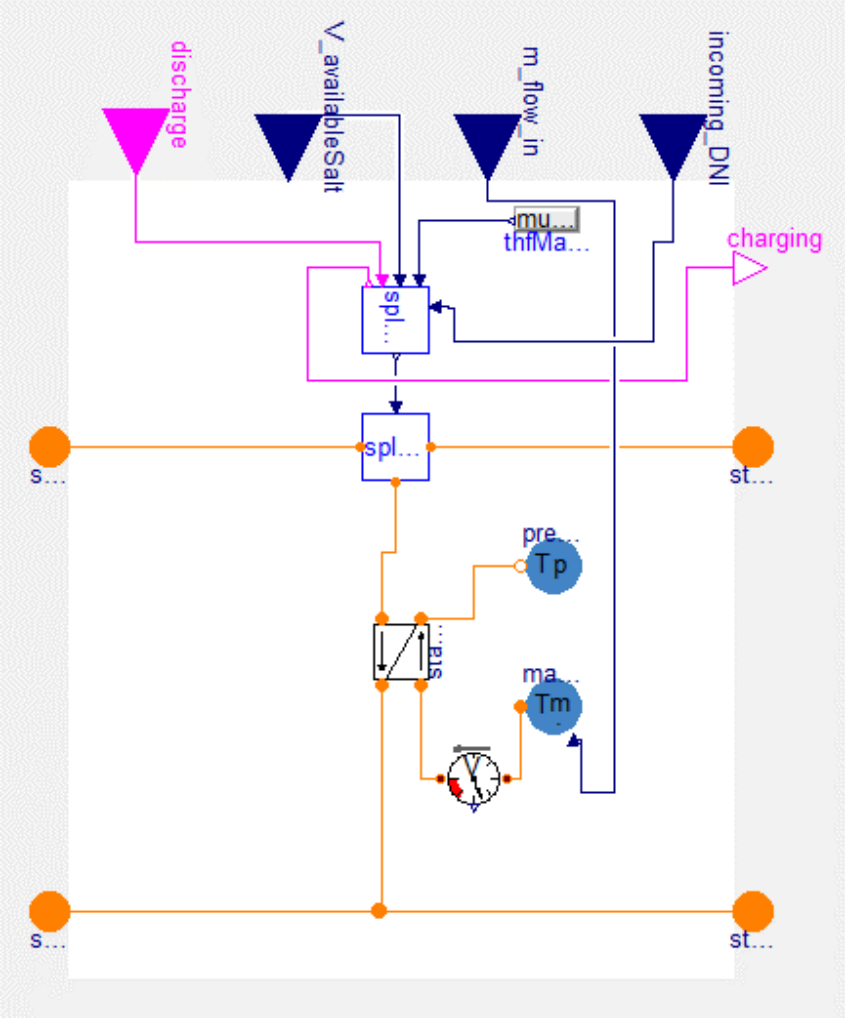

Figure 22 Model responsible of charging the thermal storage inside the thermal storage model.

7.3.3.2 Discharging the thermal storage

The discharging of heat from the thermal storage is a bit more complicated. When this is done the collector field is shut off via valves creating a new loop for the thermal heating fluid that runs through the thermal storage and then to the power cycle. This isolates the main thermal fluid pump creating the need for a secondary pump that is only used when discharging the thermal storage. The mass flow rate of this pump is calculated for the new power cycle thermal heating fluid inlet temperature of 373 °C.

$$\dot{m}_{THF,sec} = \frac{\frac{Q_{turbine}}{\eta_{powercycle}}}{h_{THF@373℃} - h_{THF@293℃}} = \frac{\frac{50 \cdot 10^6}{0.388}}{731327 - 539200} = 670.7\, kg/s$$

The threshold value of incoming solar irradiation can be set by the user and all simulations in this thesis uses the value of 400 W/m^2which means that the system will switch over to run on the thermal storage when the DNI is less than this value. The value has been chosen after tests and is not calculated.

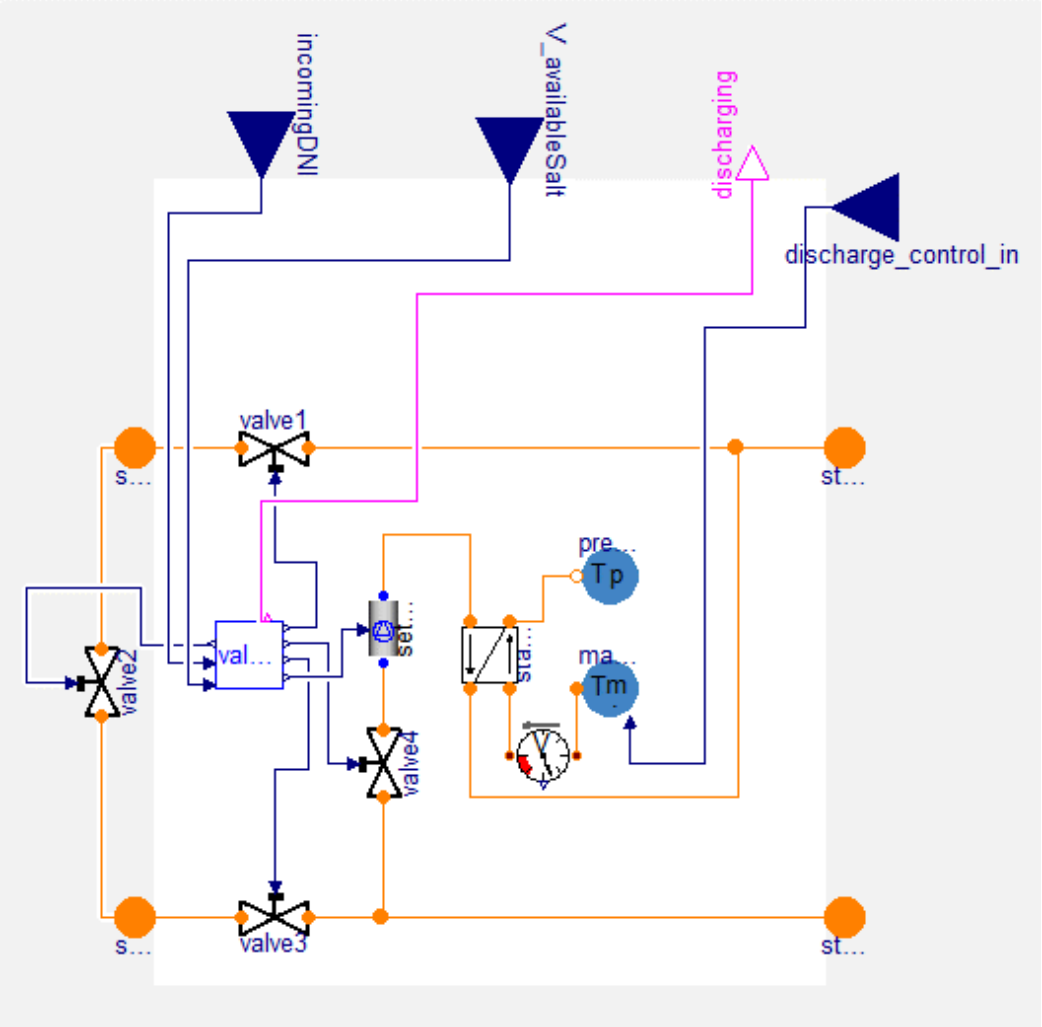

Figure 23 Model responsible for discharging of the thermal storage inside the thermal storage model. Valve 2 shuts off the collector field loop.

7.3.3.3 Simplifications made to the thermal storage model

When building the thermal storage model in Dymola two simplifications have been made. The first one is to divide the model in two sub models, one taking care of the charging and the other one taking care of the discharging. This means that the system has two heat exchangers instead of one and a double set of cold and hot storage tanks. The main reason for this is to simplify the control structure for the model. The other simplification is that the models do not incorporate any real tanks but uses a sink and source of molten salt instead. The volume flow rate of solar salt is then measured in order to keep track of how much salt is heated up by the system and vice versa. This means that there is no risk of using more than maximum available salt in a simulation. If only one set of tanks were to be used a rather tricky control problem would be introduced. The control system then needs to keep track of which tank contains hot and cold salt and from which tank to pump when heating up the system versus heating up the salt. With this simplification the system knows how much hot and

cold salt is available at any given time and also which valves and pump that should be altered when a specific task, charging or discharging, is to be performed.

7.3.4 Power cycle

The power cycle including boiler, steam turbine, generator and condenser is modeled very simply due to shortage of time. The Rankine power cycle model consists of a single heat exchanger where the thermal heating fluid is running on the primary side and the water boiled to steam on the secondary side. The water is supplied from a source and dumped in a sink meaning that there is no turbine, generator or condenser model. By using this only heat exchanger the thermal inertia of the otherwise big boiler is not accounted for. This mean that the system modeled in Dymola will react very fast to changes in incoming thermal fluid temperature.

An automatic control circuit controls the outlet temperature of the THF from the boiler to keep it constant at 293 °C which is the temperature the thermal heating fluid should have when returned to the collector field. Calculations on how much heat that should be supplied to the power cycle can be carried out because the total efficiency of the steam cycle in the Andasol plant is known and is assumed to be the same in the model in Dymola. The total efficiency of the power cycle is known to be 38.8 %, and this efficiency is used in calculations made on the model. If a more detailed Rankine cycle is added later with another total efficiency than used in this thesis some calculations in the validation chapter must be redone. This is stated later on in the report.

7.3.5 Control

The control system consist of four automatic control regulators all regulating mass flow rate and one control unit for the dumping of absorbed heat by intentionally defocusing a part of the collector field.

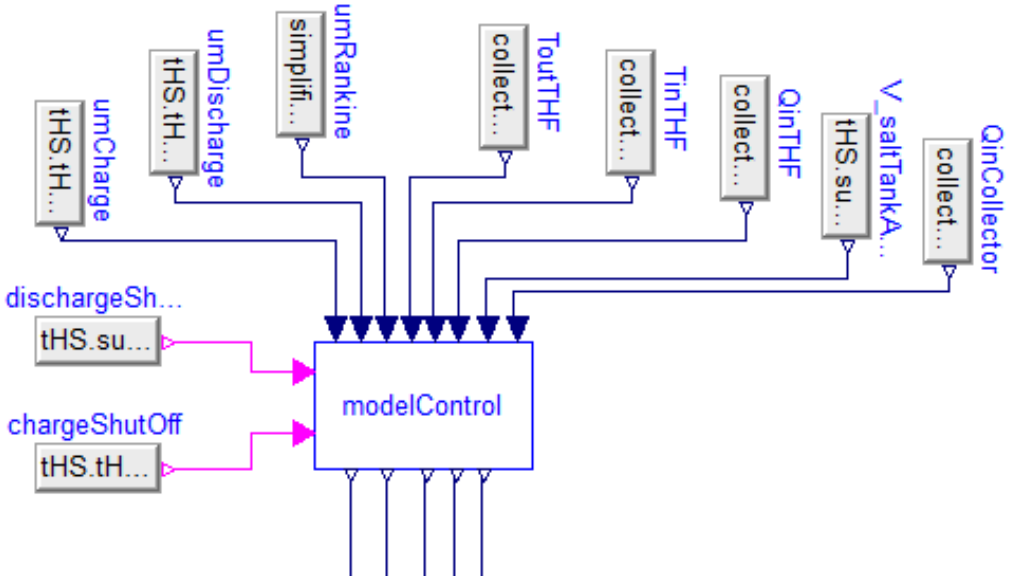

Figure 24 Overview of the control unit in the detailed system in Dymola.

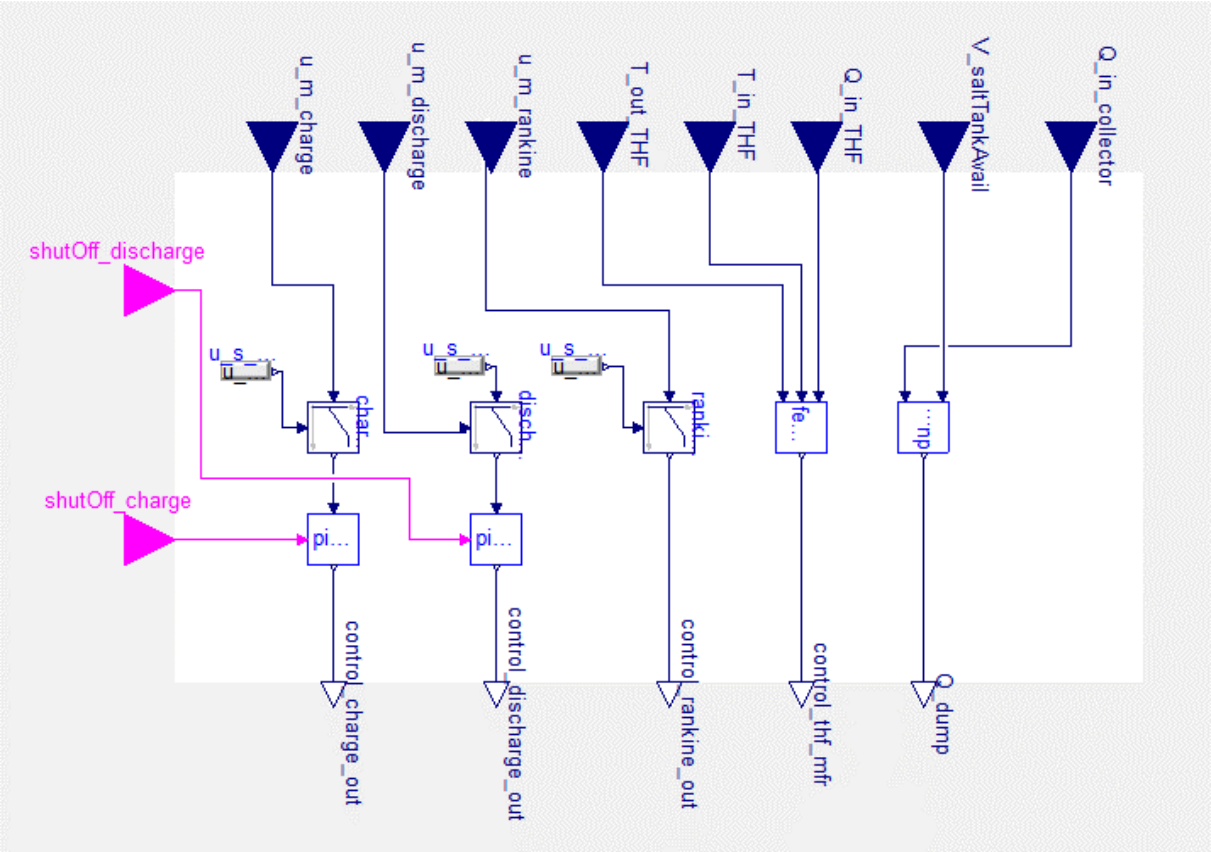

Figure 25 The inside of the control unit for the detailed system. It consists of three PI regulators, a feed forward controller and a control unit calculating the amount of heat to dump.

7.3.5.1 Thermal heating fluid pump control

This automatic control regulator unit makes sure that the thermal heating fluid outlet temperature form the solar collector field is kept as close to the desired 393 ℃ as possible. This is done by regulating the thermal heating fluid mass flow rate through the collector field. The regulator consists of a feed forward control unit calculating the desired mass flow rate at the current concentration of solar irradiation onto the receiver. The feed forward design was chosen to eliminate fluctuations of the mass flow rate and to get a more stable regulator. The thermal heating fluid outlet temperature from the collector field is set very close to the maximum fluid temperature which demands an accurate regulator of the mass flow rate to avoid overheating the fluid. If the fluid were to be overheated it may deposit solids on the heating surfaces being the inside of the receiver steel pipe.

The desired mass flow rate in the feed forward regulator is calculated as following:

$$\dot{m}_{THF,ff} = \frac{Q_{receiver} - Q_{env,conv} - Q_{env,rad}}{h_{THF@393℃} - h_{THF@292℃}} \qquad (35)$$

This feed forward calculation is not possible in a real system where measuring the losses would be impossible.

A standard PI-regulator is the measuring any deviations from the desired output temperature in order to reduce any error and the signal from the PI-regulator and the feed forward regulator is added up and sent to the pump.

7.3.5.2 Thermal storage control

The thermal storage control consists of two PI-regulators controlling the mass flow rate of solar salt. The charging control unit is used when the thermal storage is charged with heat. The system measures the salt outlet temperature from the heat exchanger and controls the mass flow rate of cold solar salt in order to deliver hot salt to the storage tank at the desired temperature of 383 ℃. The second PI-regulator controls the mass flow rate of hot salt when the thermal storage is delivering heat to the thermal fluid. The thermal fluid outlet temperature from the heat exchanger is measured in order to control the mass flow rate of salt to keep the outlet temperature at the desired level of 373 ℃.

Inside the thermal storage unit model there is a separate control box for each sub component, the charging and discharging heat component to the thermal storage. These control boxes controls valves and pumps in order to redirect flows and tapping of hot oil to the thermal storage and deliver heated oil to the Rankine cycle.

7.3.5.3 Dump control

The solar collector field of the Andasol power plant is over-dimensioned in order to be able to deliver heat both to the Rankine cycle and the thermal storage. This means that too much heat is delivered to the Rankine cycle when the thermal storage is fully loaded and a part of the absorbed heat has to be dumped. This is done by stowing, intentionally defocusing, a part of the collector field and thereby absorbing less heat to the thermal heating fluid. The dump control calculates how much heat that should be dumped in the case of the thermal storage being fully loaded and too much heat is absorbed. This information is then passed on to the mirror component that calculate how many percent less heat that should be absorbed compared to the current amount of heat being absorbed.

$$Q_{dumped} = Q_{absrober} - \frac{Q_{turbine}}{\eta_{powercycle}} \quad [W] \qquad (36)$$

This means that a very exact amount of heat can be dumped. In a real system it's only possible to stow complete collector assemblies that means that a little too much or too little heat than needed will be dumped. Another problem with this design is that not all of the concentrated heat on to the receiver is absorbed by the thermal heating fluid, some is lost by radiation and convection from the receiver. This means that too much heat is being dumped with this control design. As a solution to this problem the measurement signal to the dump control is reduced with 5 percent that is roughly the total amount lost to convection and radiation during normal operation compared to the amount of heat concentrated on to the receiver.

7.3.5.4 Rankine cycle control

The Rankine control unit consists of a PI-regulator controlling the mass flow rate of water boiled to steam in order to deliver thermal heating fluid back to the collector field at the desired temperature of 293 ℃. This is done by measuring the thermal heating fluid outlet temperature and controlling the mass flow rate of water on the steam side of the heat exchanger.

7.4 SYSTEM MODELS

When the solar power specific components have been implemented in Dymola they are put together to a complete system that will be presented below.

7.4.1 Simple system model

The simple system model is connected together as shown in Figure 26. The thermal heating fluid main pump is placed just before the collector field and controlled with the pump control unit. The heated thermal fluid leaves the collector field and can either be sent to the Rankine cycle or the oil is bypassed and redirected back to the collector field if the thermal fluid has a lower temperature then the desired 393 °C. The bypass control unit controls the bypassing of oil. An expansion vessel of 2 m^3 is placed after the Rankine cycle to handle volumetric changes of the thermal fluid.

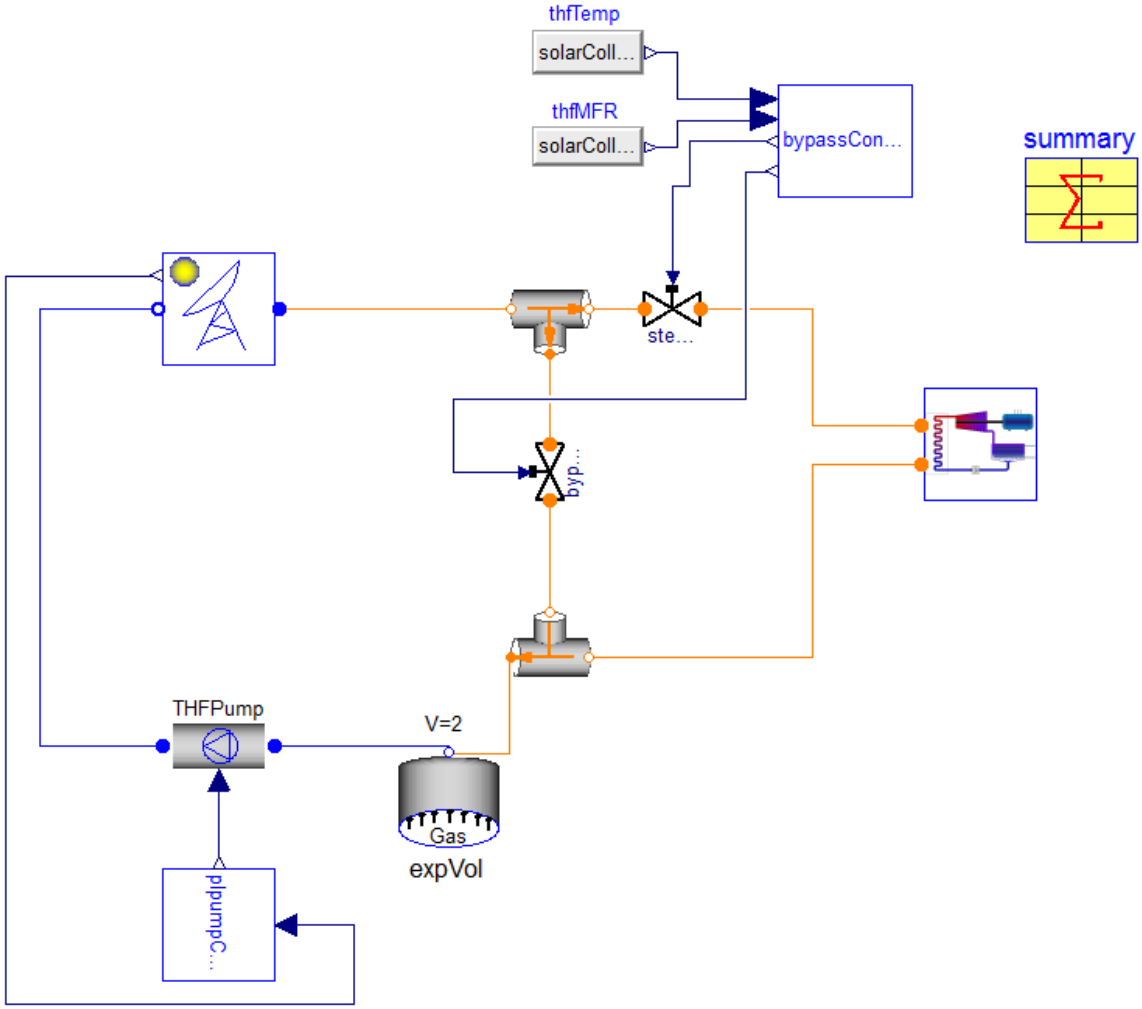

Figure 26 Overview of the simple system model.

7.4.2 Detailed system model

The detailed system model is composed in almost the exact same way as the simple system model but have a couple of more models as seen in Figure 27. The sun model is connected to the collector field model and outputs the amount of solar irradiation hitting the aperture perpendicular to the aperture normal. After the collector field the thermal storage is connected. The heated thermal fluid can be tapped off to heat up the thermal storage or the collector field and main thermal fluid pump can be shut off. This happens when heat is discharged from the thermal storage and the second thermal fluid pump is started. The control unit houses all the regulators for pumps and the dump control unit.

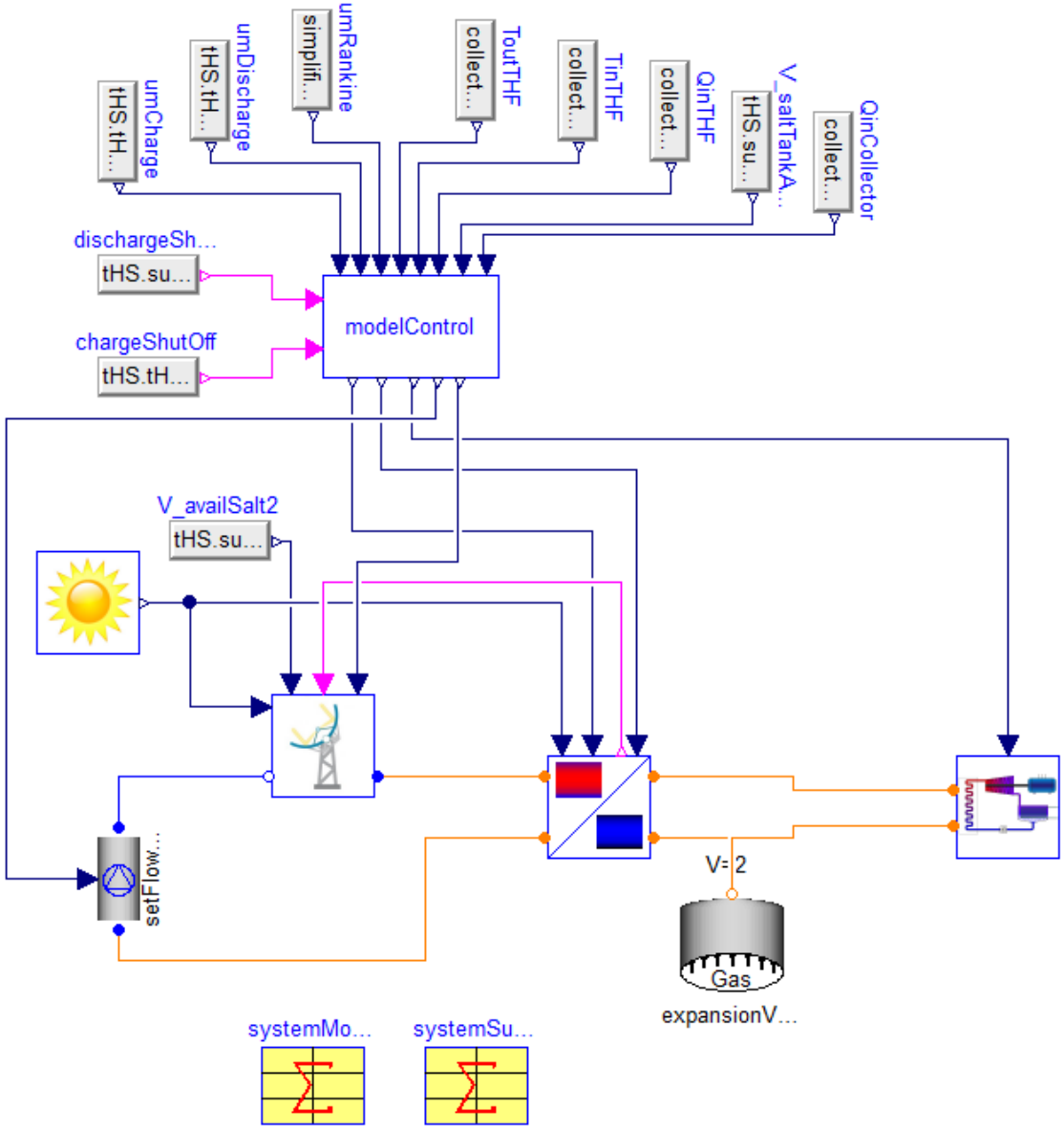

Figure 27 Overview of the detailed system model.

8 VALIDATION OF COMPONENT AND SYSTEM MODELS

An important part of modeling is to validate if the models actually align with real data measurements. If that's the case the mathematics describing the component is correct and any approximations are valid. The tricky part is to find data from measurements of real systems and to adapt the model to the conditions that was set up when the data were collected.

In this case power plant owners are not very keen on giving out or publish specific data from their plants. This is because companies compete with each other on different contracts and do not want to show competitors the capabilities of their specific system. It's also hard to know how specific values like efficiencies are calculated and measured but in most cases it is peak values at design point conditions. This is because plant owners want to show as high values of example plant efficiency as possible when competing for a contract on building a new concentrating solar power plant.

8.1 STEADY STATE VALIDATION OF COMPONENTS

One of the most important and complex models is the solar collector. It consists of a series of different thermal components with heat flowing through different materials like glass, metal and through vacuum. There is also different loss models including radiation, natural convection and forced convection. This means that this model is very sensitive to errors and should be validated in order to make the different data outputs form the component like efficiency credible.

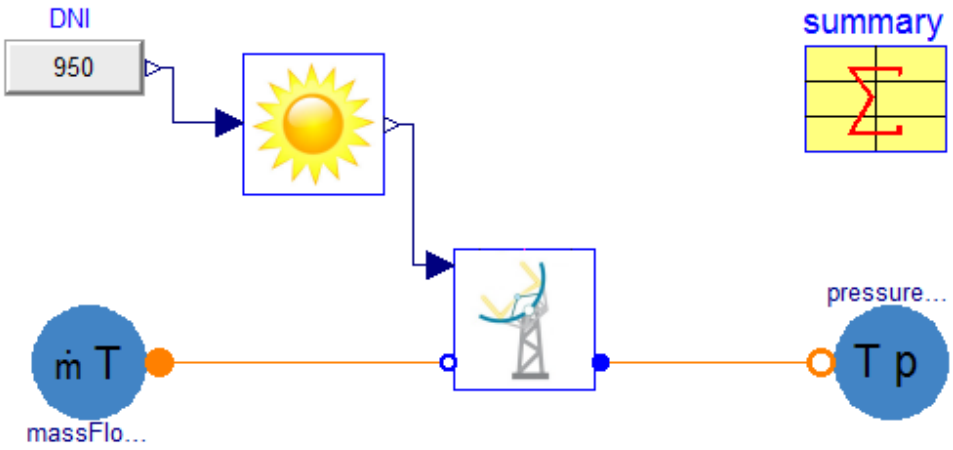

Figure 28 Overview of the steady state system used for one-dimensional validation.

A one dimensional, steady state model of a parabolic trough receiver was developed and simulated by Dudley et al and Forristall. This model is also validated by experimental data from testing of the receiver used both in Andasol and in this thesis, the Schott-RP 70. Results from a sensitivity study of this model are compared with an equal of the receiver implemented in Dymola. In Table 8 below three different cases are presented with the specific parameter values used. [26]

Model inputs	Case 1	Case 2	Case 3
I_b	950 W/m^2	950 W/m^2	950 W/m^2
θ	20°	0°	45°
w_{ap}	5.75 m	5.75 m	5.75 m
η_{opt}	0.75	0.75	0.75
$\dot{m}_{THF}$	7.6 kg/s	8.1 kg/s	5.1 kg/s
T_{THF}	340 ℃	340 ℃	340 ℃
T_{amb}	30 ℃	30 ℃	30 ℃
Wind speed	2.5 m/s	2.5 m/s	2.5 m/s
$\varepsilon_{abs,pipe}$	0.086	0.086	0.086
$\varepsilon_{abs,env}$	0.89	0.89	0.89

Table 8 Parameter settings for the three different steady state test cases

8.1.1 Results

The results from each case study are presented in Table 9 below together with the values from the technical report.

Model outputs	Case 1 - paper	Case 1 - Dymola	Case 2 - paper	Case 2 - Dymola	Case 3 - paper	Case 3 - Dymola
$Q_{abs,THF}$ $[W/m]$	3690	3686.9	3953	3949.2	2471	2468.4
$Q_{loss,rad}$ $[W/m]$	76	71.83	78	73.5	68	64.2
$Q_{loss,conv}$ $[W/m]$	150	158.75	154	163.1	132	138.6
$Q_{loss,tot}$ $[W/m]$	226	230.58	232	236.6	200	202.8
$\boldsymbol{\eta_{th}}$	0.675	0.675	0.724	0.723	0.452	0.452

Table 9 Results from the steady state test cases.

The thermal efficiency of the receiver is calculated as following:

$$\eta_{th} = \frac{Q_{abs,THF}}{Q_{irradiation}} \qquad (37)$$

$$Q_{irradiation} = L_{rec,tot} \cdot w_{ap} \cdot I_{b,0} \qquad (38)$$

Where $I_{b,0}$ is the insolation on the trough aperture at zero incident angle without being scaled by $\cos\theta$. [26]

The results shown in Table 9 indicate that a correct implementation of the receiver has been done. The small difference in heat loss is because the model used to conduct the calculations in the paper doesn't include convection in the vacuum space between the absorber pipe and glass cover. A small amount of heat is transferred via molecular convection and therefor a greater heat loss to the ambient air takes place in the model implemented in Dymola.

No other components than the receiver were tested because of the lack of data to compare any results from Dymola with.

8.2 STEADY STATE VALIDATION OF SYSTEM MODEL

To validate the system as a whole a comparison with the Andasol I parabolic trough power plant located in Aldeire y La Calahorra, Spain is carried out with specific design parameters listed in Table 10. The goal is to match efficiencies from different parts of the system with supplied efficiencies from the Andasol solar power plant. The difference between this system and the system in the previous test is that the simplified Rankine model is connected and the THF flows like in the real power plant controlled by a pump. This model also uses the sun model developed with tracking capabilities of the collector assemblies to minimize the solar irradiation incidence angle to the normal of the collector aperture. It's basically the complete detailed system model but without the thermal heat storage which is being modeled in this validation. The thermal storage will not be used in this validation test, neither for heating up the salt or to heat up the thermal fluid. It's left out from the simulation due to efficiency calculations that will turn out wrong if heat is added or subtracted from the system.

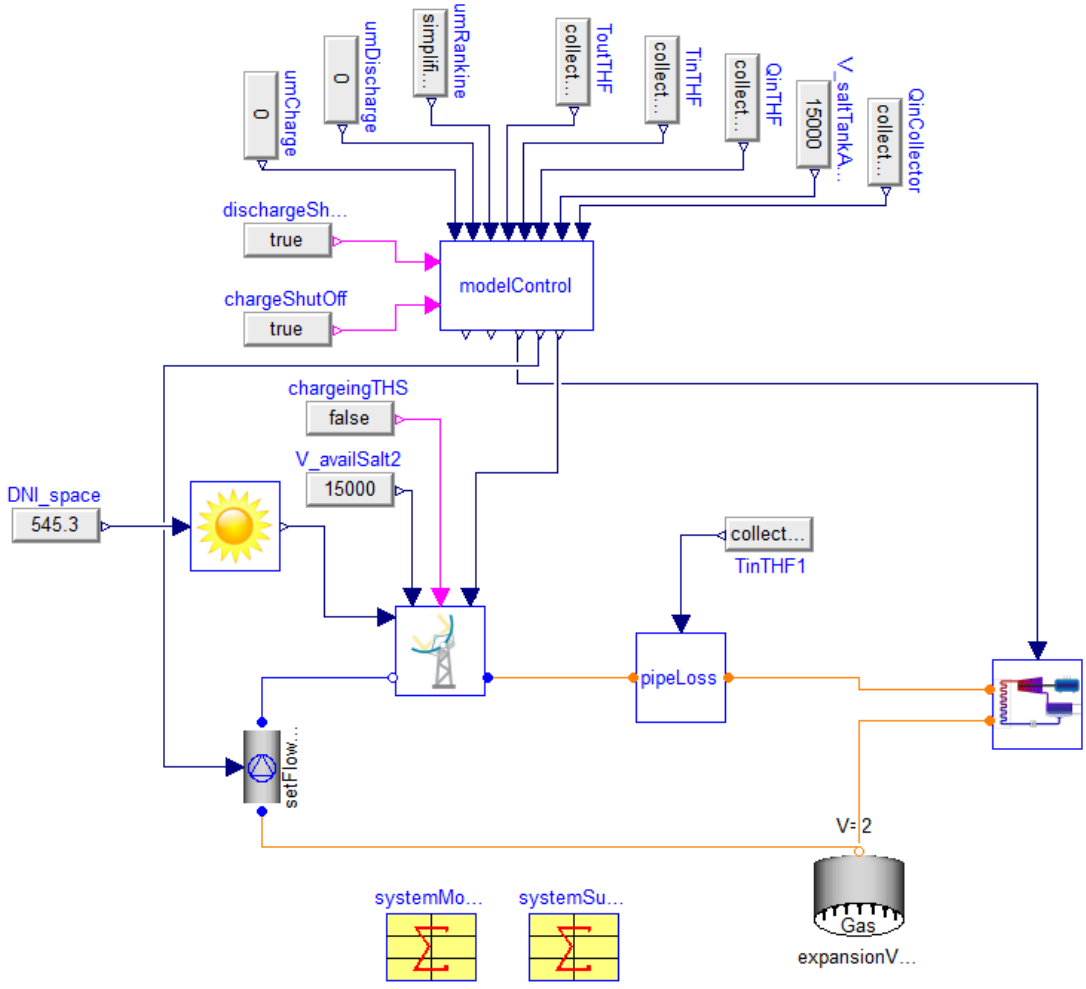

Figure 29 Overview of the system model used for the Andasol validation tests.

The different efficiencies from the Andasol power plant is based on yearly average solar irradiation and power production. In order to make a correct simulation the parameters regarding incoming solar irradiation must match a yearly average on this location. The solar data used are based on a

typical metrological year from weather data over a 19 year long period. [28] An average value of the solar irradiation is calculated as following:

$$DNI_{avg} = \frac{\sum_{i=1}^{365} DNI_i}{365 \cdot t_{avg}} \qquad (39)$$

Where t_{avg} is the average amount of solar hours per day. The average amount of solar hours per day is set to 9.5 hour giving an average value of the direct normal irradiation:

$$DNI_{avg} = 545.3 \ W/m^2$$

To calculate the correct angle for the tracking mechanism for the solar collector the day of the year and the time of the day is also needed. These were chosen to represent an average value like spring or autumn. [15] [29]

	Andasol I	Model in Dymola
Total receiver length	89856 m	89856 m
Aperture width	5.67 m	5.67 m
Glass envelope outer diameter	0.125 m	0.125 m
Glass envelope inner diameter	Unknown	0.115 m
THF steel pipe outer diameter	0.07 m	0.07 m
THF steel pipe inner diameter	Unknown	0.064 m
Heat transfer coefficient for vacuum gap	Unknown	0.000115 W/m^2K
Absorber glass cover surface emissivity	Unknown	0.8
Absorber tube surface emissivity	0.095	0.095
Pipe system efficiency	Unknown	0.97
Day of the year	Unknown	92
Time of day	Unknown	10 AM
Longitude	-3.071° west	-3.071° west
Latitude	37.2308° north	37.2308° north

Table 10 Parameter settings used for the Andasol validation tests.

There is a range of other parameters that could be varied to test the specific parameter impact on the system. Therefor a sensitivity study is carried out to with a set of different parameters that is listed in Table 11.

Taste case number	Optical efficiency	Wind speed [m/s]	Number of nodes	Ambient temperature	Direct normal irradiation

				[°C]	$[W/m^2]$
1	0.7	0	5	20	545.3
2	0.9	0	5	20	545.3
3	0.7	2.5	5	20	545.3
4	0.7	0	10	20	545.3
5	0.7	0	5	35	545.3
6	0.7	0	5	20	700

Table 11 Different test cases set up for the sensitivity study for validation against performance numbers given by Andasol.

8.2.1 Results

The results from the sensitivity study are compared with values of system efficiencies provided by Andasol for the Andasol-I solar power plant in Table 12. [30]

Efficiency	Andasol	Dymola – case 1	Dymola – case 2	Dymola – case 3	Dymola – case 4	Dymola – case 5	Dymola – case 6
Solar field – solar irradiance to steam	43 %	42.6 %	43.4 %	42.7 %	42.0 %	42.6 %	33.8 %
Rankine – steam to electricity	38.8 %	38.8 %	38.8 %	38.8 %	38.8 %	38.8 %	38.8 %
System – solar irradiance to electricity	16 %	16.5 %	16.8 %	16.5 %	16.6 %	16.5 %	13.1 %

Table 12 Results from sensitivity study compared with numbers given by Andasol.

The pipe system efficiency is set to 97 % meaning that there is a 3 percent loss in the piping system coming from the collector field going to the power block where the boiler, turbine, condenser and solar salt tanks are located. The collector field is very large, in the Andasol case approximately 500000 square meters, which in some cases means that the heated thermal fluid is pumped through long pipes. These pipes are insulated but it's implied that some loss occur and considering the high temperature of the fluid and the high mass flow rate a 3 percent loss seems reasonable.

Solar field efficiency is calculated as following:

$$\eta_{solarfield} = \frac{\dot{Q}_{boiler,in}}{I_b \cdot L_{rec,tot} \cdot w_{ap}} \qquad (40)$$

Rankine efficiency is the whole Rankine cycle efficiency including the condenser. In this thesis only a simplified version of the Rankine cycle is used meaning that the efficiency provided by Andasol will be used to calculate the amount of electricity produced for the system modeled in Dymola.

The solar irradiance to electricity efficiency is calculated as following:

$$\eta_{system} = \frac{\dot{Q}_{boiler,in} \cdot \eta_{Rankine}}{I_b \cdot L_{rec,tot} \cdot w_{ap}} \qquad (41)$$

If a detailed Rankine cycle is added later with another total efficiency then 38.8 % the solar irradiance to electricity efficiency must be recalculated.

As shown in Table 12 the model in Dymola aligns well with values from the real system and when looking at the result from the sensitivity study there is little or no difference between most of the parameter changes. The parameter that gives the biggest impact is the direct normal irradiation. When more radiation hits the collector more heat can be absorbed to the thermal fluid but at the same time there is a maximum value of how much steam that can be produced and sent to the turbine for electricity production. Looking at the equation [40] for the solar field efficiency the numerator is basically constant and increased direct normal irradiation the denominator increases which decreases the efficiency.

8.3 DETAILED LIST OF LOSSES

To get an overview of the losses from the system and where in the system they occur a detailed list of the different losses in the system is made. To compose the list values from case number one from the sensitivity study made above in the system model validation is used. Dumping is listed as a loss that occurs just before solar irradiation hits the mirror that is not an entirely correct interpretation. Dumping is made because the solar field is over-dimensioned in order to produce heat to the power block and the thermal storage. In this case the thermal storage is disconnected from the system and dumping is made in order to deliver the correct amount of heat to the power block. If dumping, intentionally defocusing a part of the collector field, is not made too much heat is delivered to the power cycle.

Part of system	In	Out	Loss	Efficiency	Total efficiency	Total loss
Solar irradiation	277.82 MW	233.34 MW	44.48 MW	83.9 %	83.9 %	16.1 %
Dump	233.34 MW	195.76 MW	37.58 MW	83.9 %	70.5 %	29.5 %
Mirror	195.76 MW	137.03 MW	58.73 MW	70.0 %	49.3 %	50.7 %
Absorber	137.03 MW	121.91 MW	15.12 MW	88.9 %	43.9 %	56.1 %
Piping system	121.91 MW	118.25 MW	3.7 MW	97.0 %	42.6 %	57.4 %
Steam cycle w. generator	118.25 MW	45.88 MWe	72.37 MW	38.8 %	16.5 %	83.5 %

Table 13 Detailed list of losses in different parts of the system.

As shown in Table 13 83.5 % of the total power from incoming solar irradiation is lost in conversion to electricity. The biggest loss in the system when not looking at the power block takes place in the mirror. There is a loss of 30 percent of the incoming solar irradiation that the mirror fails to focus on to the receiver because of mirror imperfections, soil and other parameters discussed earlier. There is

also a rather big loss from the incoming solar irradiation meaning that the mirror cannot minimize the angle between the aperture normal and the direct solar beam enough. This is probably due to the fact that the current day the simulations take place is in spring or autumn and the north to south axis tracking mechanism is optimized for summer.

The biggest loss looking at the whole system takes place in the steam cycle, which include boiler, steam turbine, generator and condenser where 61.2 percent of the power supplied from the thermal heating fluid is lost in conversion to electricity.

9 RESULTS FROM TEST CASES

The results are based on different case scenarios where the system is simulated for a day for different parts of the year. This is done to study the effects of high and low amount of incoming solar irradiation and how the system behaves under these conditions. The results are presented in a graph where heat flows to and from different parts of the system are plotted together. The system parameters are the same as from the system model validation test case number one. The direct normal irradiation is based on weather data from the specific date on which the simulation takes place.

9.1 TYPICAL CLEAR SUMMER DAY

Flabeg, the manufacturer of the solar collector assemblies for the Andasol power plant is demonstrating the performance of the plant for a typical clear summer day in Figure 30. [31] This figure gives a hint of how the system model in Dymola should behave under similar conditions. The system model is set up to run on day 189 which is 8th of July, in the middle of the year and the simulation will start at 4 AM and will run for 24 hours to be able to match the plotting with the ones provided by Flabeg. The result is presented in a similar way as the graph from Flabeg in Figure 30 below and all results from the different test cases will be presented in this way.

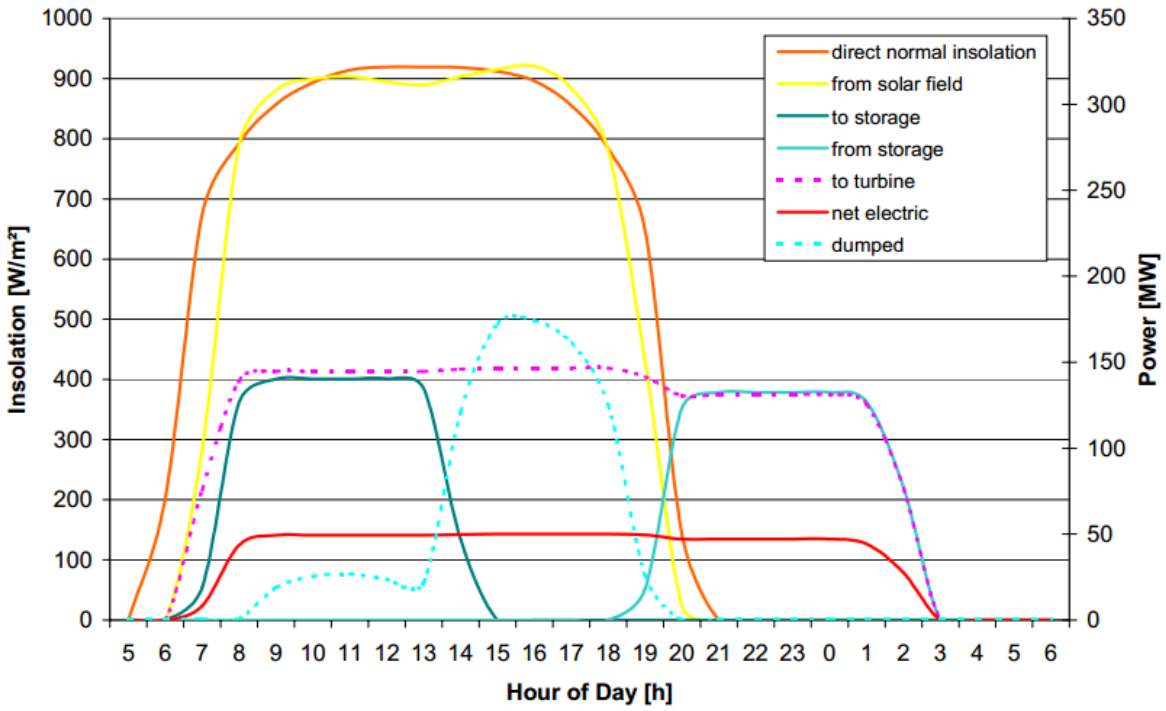

Figure 30 Graph of heat flow to and from different parts of the system for the Andasol power plant.

As seen in Figure 32 the simulation in Dymola is a bit rougher with sharper edges than the presented graph from Flabeg. The most obvious reason for this is that the graph from Flabeg is a computer rendering and is not based on actual calculations that are the case for the graph generated by Dymola. There is a problem with the automatic control circuit causing the fluctuations in the beginning of the day for the simulation. This could be avoided if the control parameters were optimized more carefully.

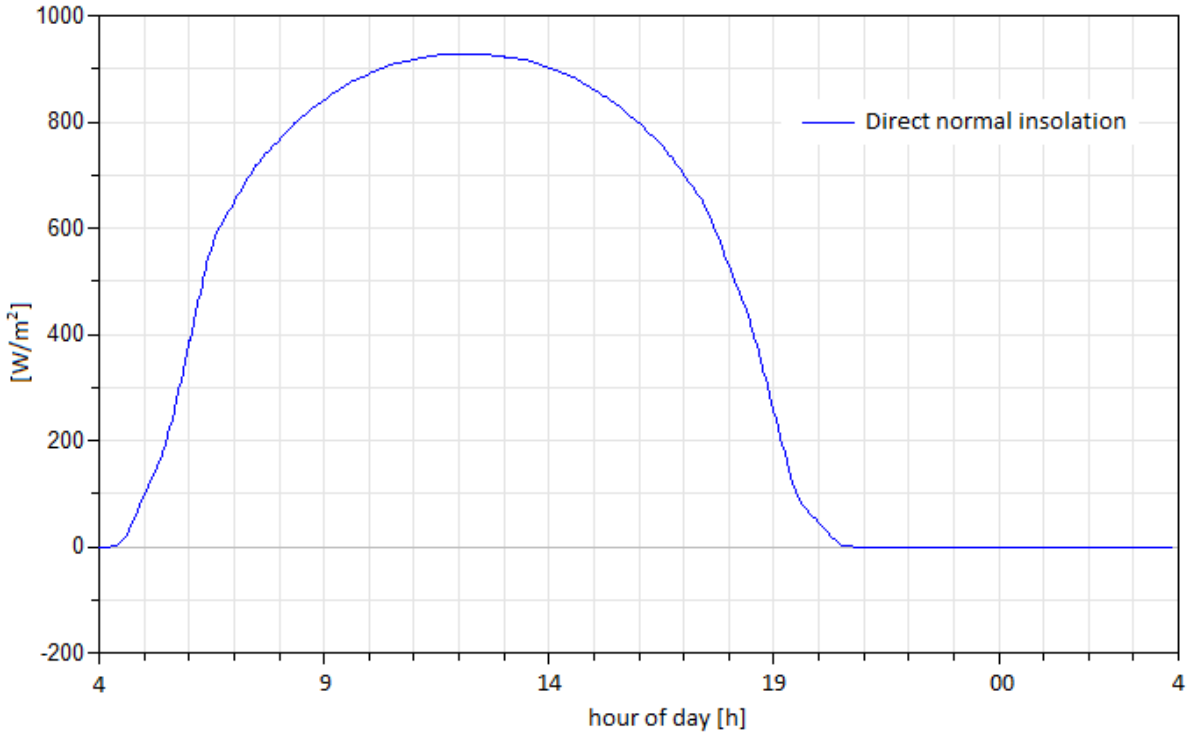

Figure 31 The direct normal irradiation for the second clear summer day simulation on the 8th of July.

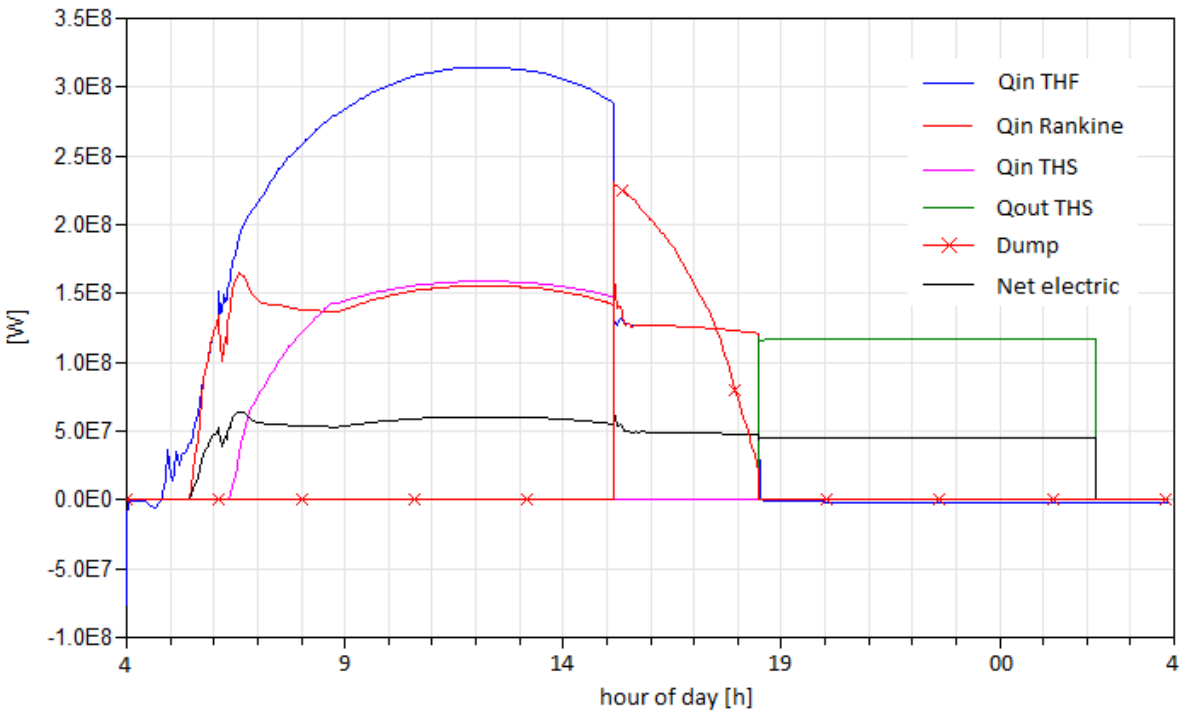

Figure 32 Heat flow in the system for the 8th of July simulation in Dymola. Simulation starts 4 AM. Different states are marked with 1, 2 and 3 in the figure.

As seen in Figure 32 the thermal storage is fully charged and the system starts to dump heat just after 3 PM. This particular day have a large amount of solar insolation causing the system model to deliver more heat than needed to the Rankine cycle even when charging the thermal storage. This is why the system model deliver more electrical power then actually possible. Just as in Figure 30 the

Flabeg system is dumping heat even thou the thermal storage is not completely fully charged. The system model does not have this future and is only dumping heat when the thermal storage is fully charged.

Beside the control problems in the beginning and the lack of dumping while charging the thermal storage the system model is behaving almost exactly as the system presented by Flabeg. One major difference is that the system model switches between states, charging and discharging heat from the thermal storage, much quicker than Flabegs' system. An explanation for this may be that the thermal inertia of the boiler is not simulated in the system model. In a real system it takes a while for the boiler to react on changes in heat input due to the large amount of steel and water in the boiler. This means for example that the mass flow rate of hot solar salt doesn't have to be max from the beginning of discharging. This could be modeled with a smooth increasing signal to the hot salt pump instead of a direct real value that is the case now. The system will behave even more like the Flabeg system if a real Rankine cycle were to be implemented to the system model in Dymola.

9.2 PARTLY CLOUDED TYPICAL SUMMER DAY

To investigate how the system behaves during a day which is partly clouded a custom set of solar data was made and parsed to the system based on the data from the typical clear summer day, day number 189. The incoming solar irradiation during the simulation is shown in Figure 33. The sudden drop in incoming solar irradiation is supposed to mimic a big cloud moving over the solar power plant. After three hours the cloud has passed and the solar irradiation goes back up again until the end of the day. The system results are shown in Figure 34.

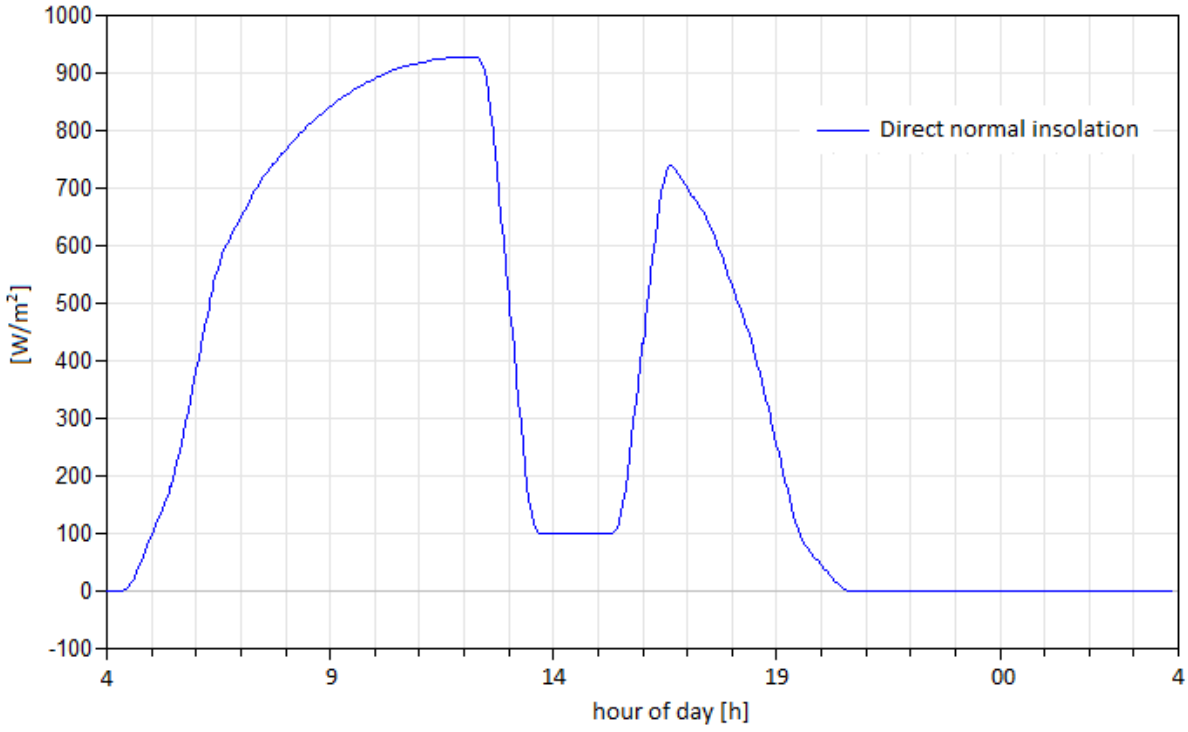

Figure 33 Direct normal irradiation for the partly clouded summer day.

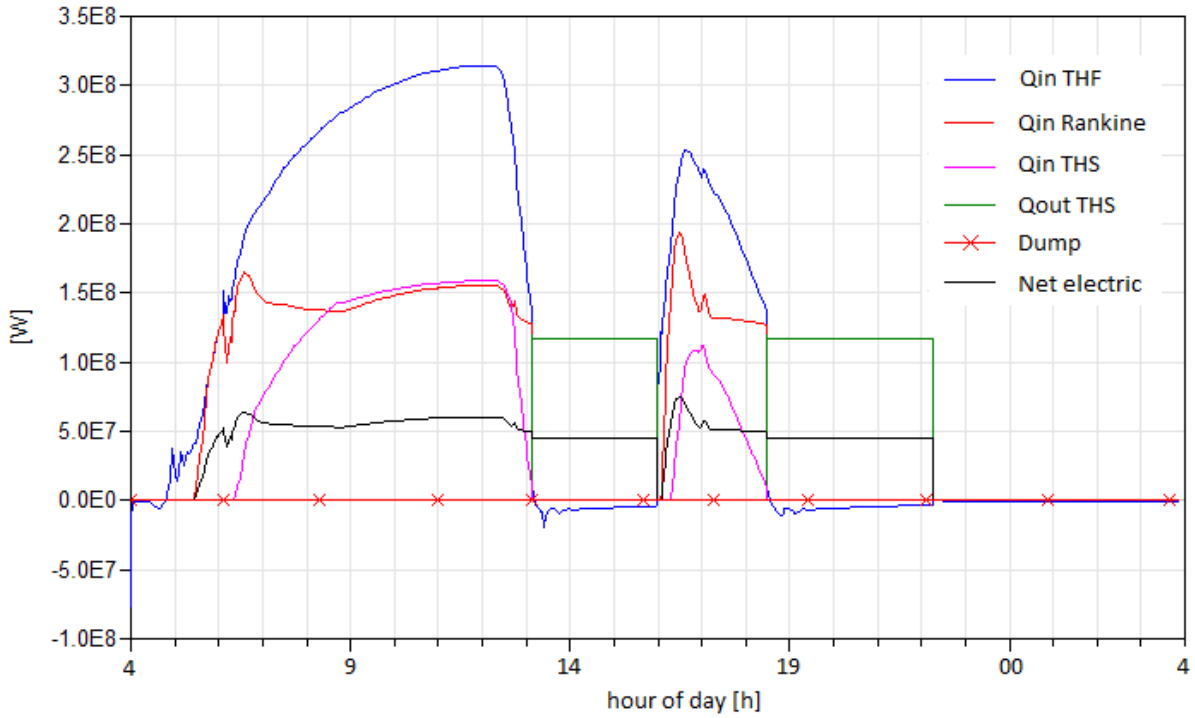

Figure 34 Heat flow from and to different system parts for the partly clouded summer day simulation. Simulation starts 4 AM.

At first the system behaves as in the clear summer day case shown in Figure 32 but when the sun is blocked by the cloud the thermal storage starts to discharge heat and the power plant can continue deliver power to the net. When the cloud passes three hours later the system switches back to run on heated thermal oil from the collector field until the sun goes down. Because of the blocking of the sun the thermal storage is not fully charged and the system can only run on the thermal storage for just little under four hours after sundown. Another control strategy may be desirable in this case depending on the price of electricity and when it's most profitable to produce it. If the electricity price is higher in the evening that it usually is the system should not start to discharge heat from the thermal storage during the day. Instead the power cycle could be shut off and started in the evening and then run on the thermal storage. In Figure 35 the tank level of the hot and cold storage tank of solar salt is shown. The cloud interrupts the charging and the system can't charge very much salt on the time left of after the cloud has passed.

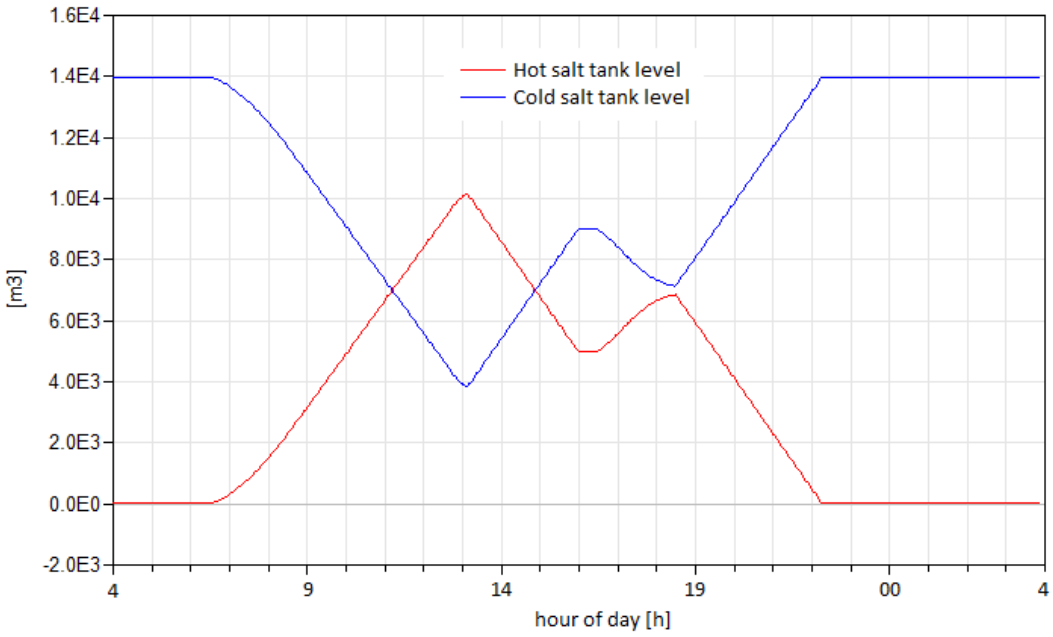

Figure 35 Hot and cold solar salt storage tank level for the partly clouded day. Simulation starts 4AM.

There is some control issue when the cloud just passes and a lot of solar irradiance hit the collector field. The system can't adjust to this large change in incoming solar irradiance fast enough that causes the power block to deliver more electricity than possible.

9.3 TYPICAL CLEAR SPRING DAY

A day spring day was chosen and simulated to study the effects of lower incoming solar irradiation. Day number 76 that is the 17th of March was simulated for 24 hours from 4 AM in the morning and the results are shown in Figure 37 below.

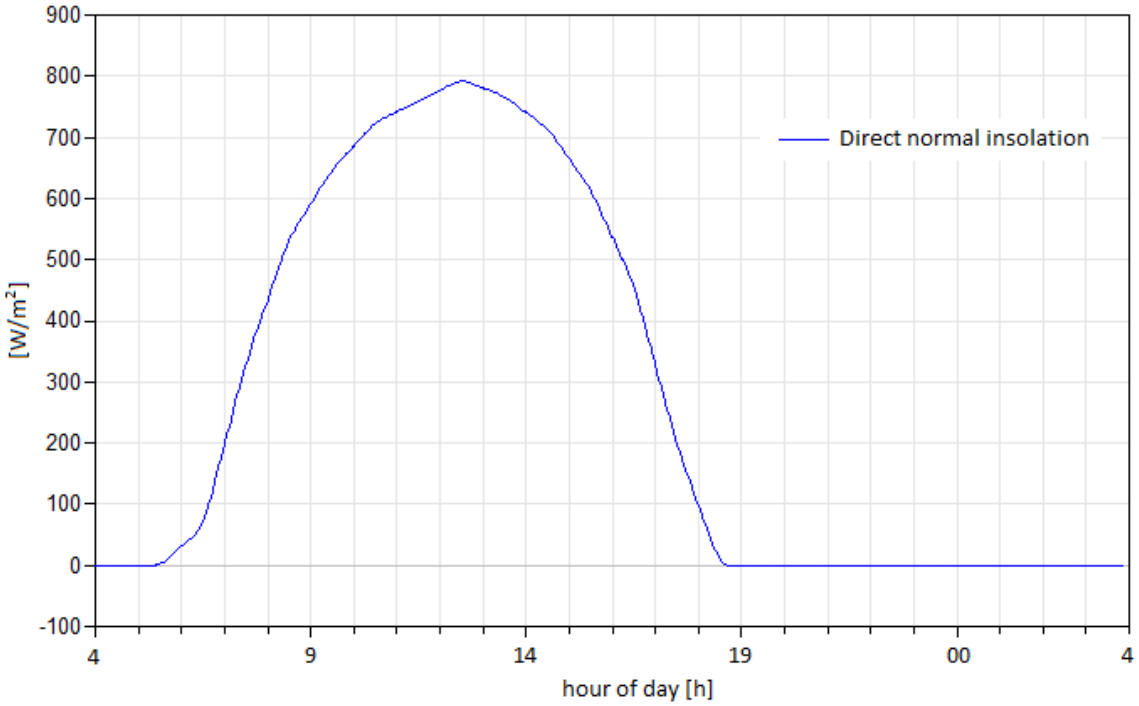

Figure 36 Direct normal irradiation for the clear spring day. Simulation starts 4 AM.

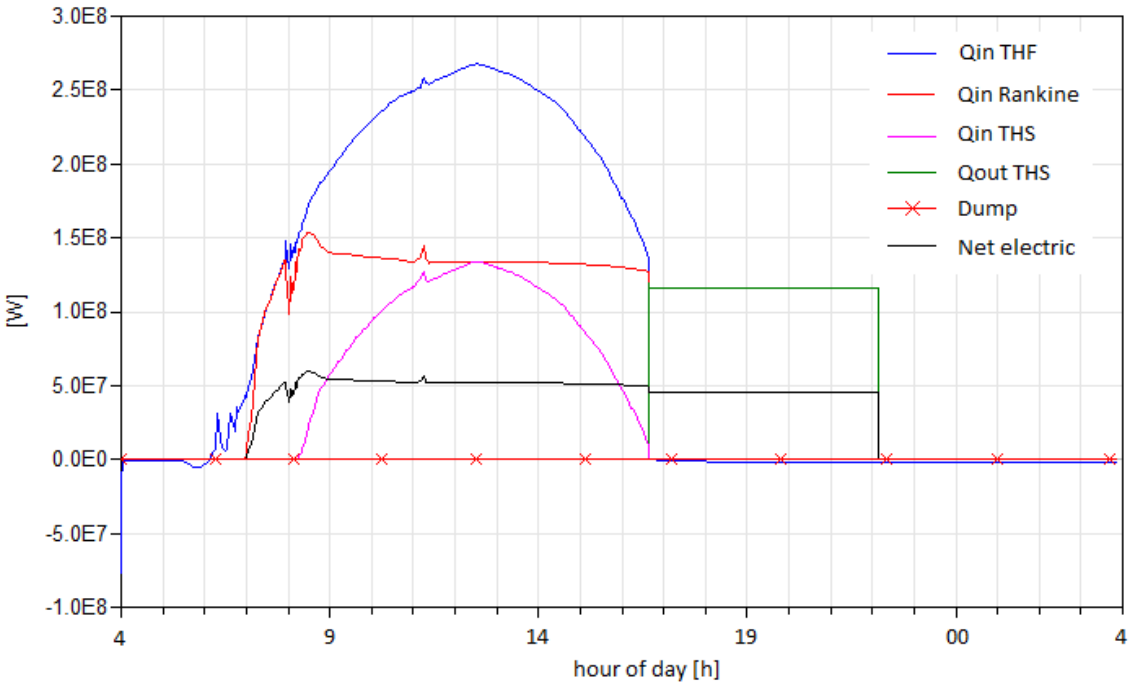

Figure 37 Heat flow from and to different system parts for the clear spring day. Simulation starts 4 AM.

Because of the low solar irradiation the thermal storage is not completely charged and the system can only run for just little over five hours of the thermal storage after sundown. Again another plant

control strategy may be wanted here were the thermal storage is discharged later in the evening if the price of electricity is higher than in the afternoon.

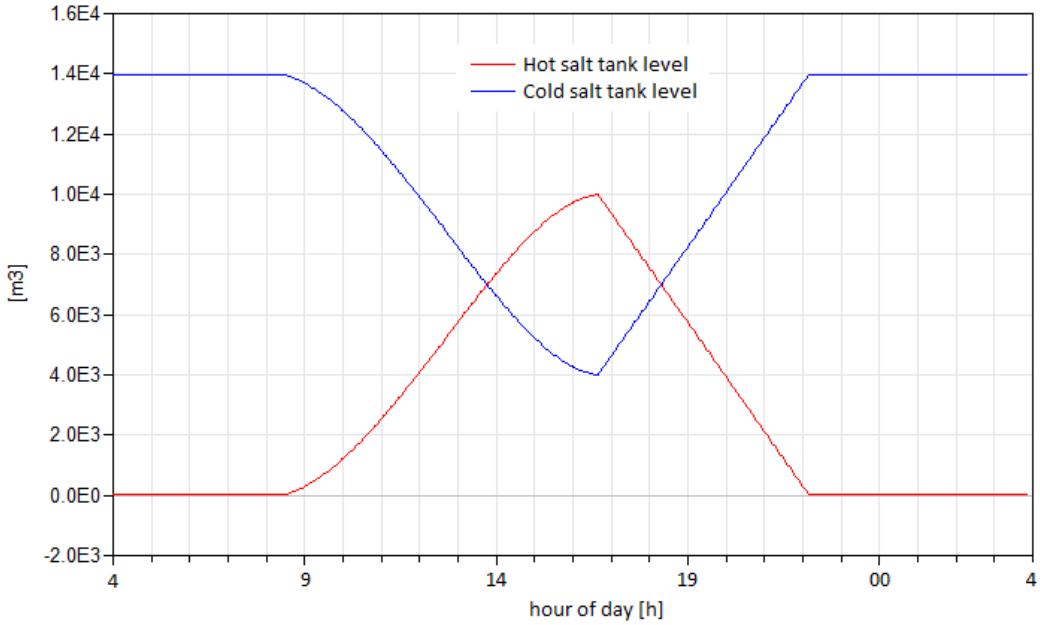

Figure 38 Salt tank levels for the hot and cold salt tank for the clear spring day simulation. Simulation starts 4 AM.

Figure 38 shows the volume of available solar salt in the hot and cold tank for the simulation during the spring day. Approximately 10000 m^3 of solar salt is heated up during an eight-hour period of the day. This is then used to run the system for little over five hours in the evening when the solar irradiation is too low to heat up the thermal heating fluid in the collector field to the desired temperature of 393 ℃. Comparing Figure 38 to Figure 35 from the partly clouded day shows that the same amount of solar salt can be charged in just six hours at the higher insolation rate which is present in the partly clouded summer day case.

9.4 TYPICAL CLEAR AUTUMN DAY

A simulation for day number 288 was made which is the 15th of October to study the effects of lower amount of direct normal irradiation during the day. The simulation started at 4 AM and was 24 hours long. As shown in Figure 39 the insolation is even lower in this simulation than in the clear spring day.

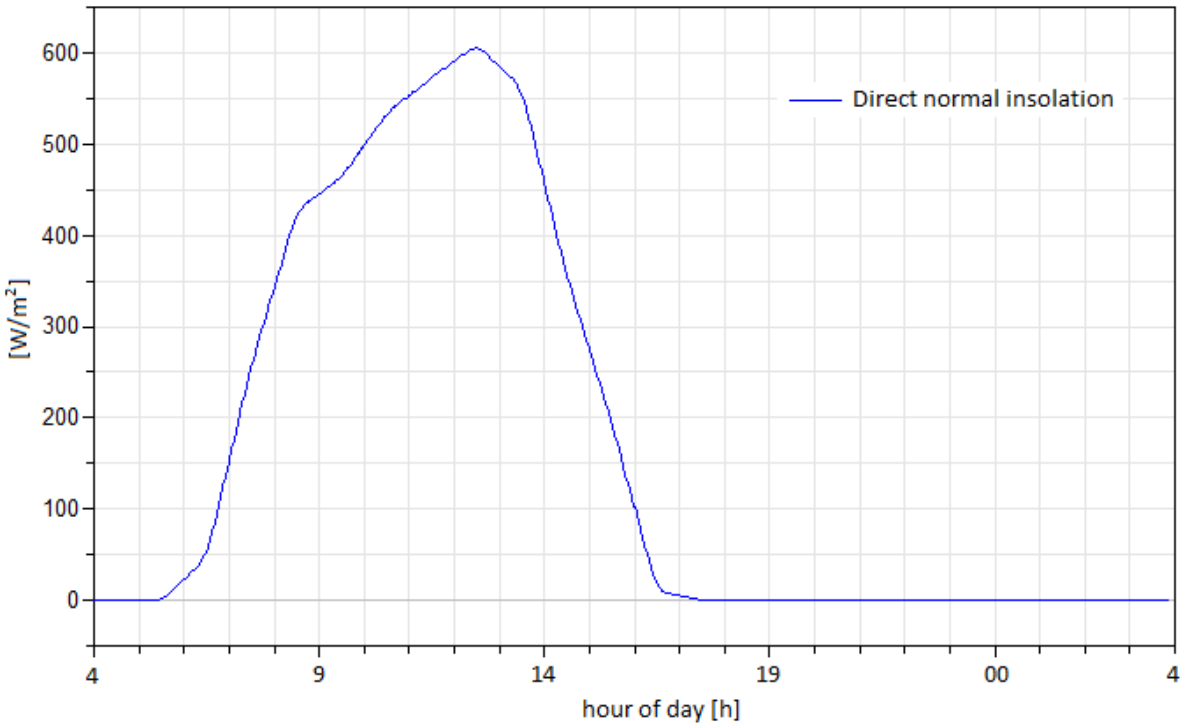

Figure 39 Direct normal irradiation for the clear autumn day. Simulation stats 4 AM

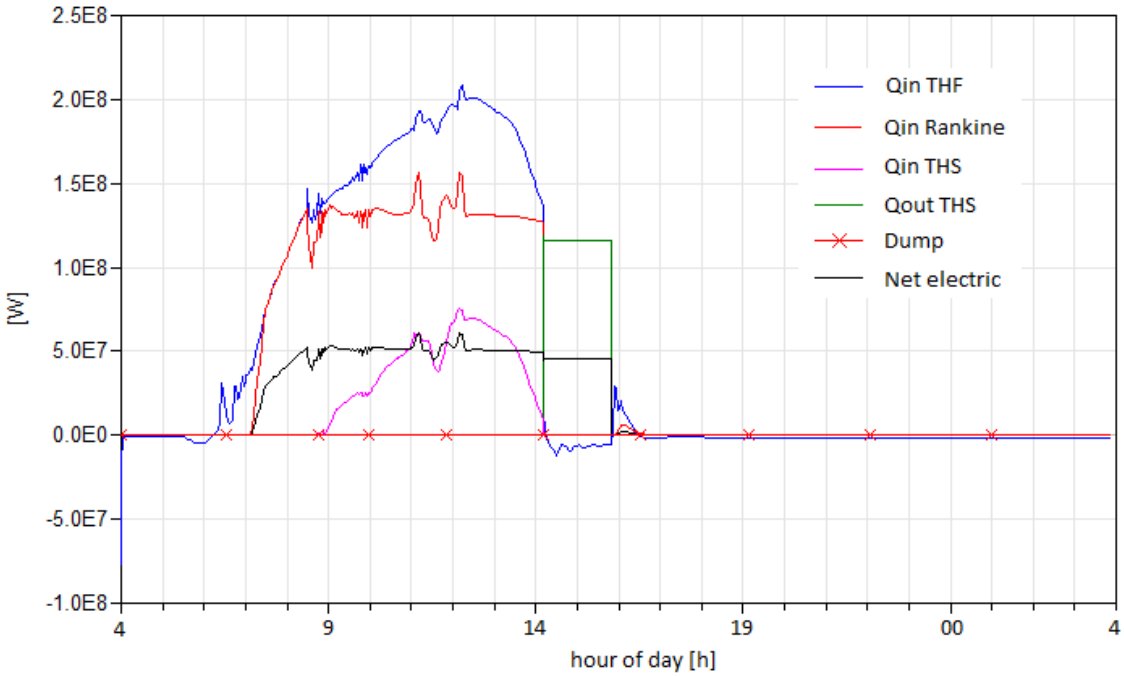

Figure 40 Heat flow from and to different parts of the system for the clear autumn day simulation. Simulation starts 4 AM.

Unfortunately the control circuit is unable to handle the variations in solar irradiation during the day that makes the spring day results in Figure 37 and the results in Figure 40 hard to compare. Very little

volume of salt is heated up and the system can only run on the thermal storage for just little under two hours. The same control parameters have been used for all test cases so far but it's clear that they have to be optimized when the insolation becomes low as in this case.

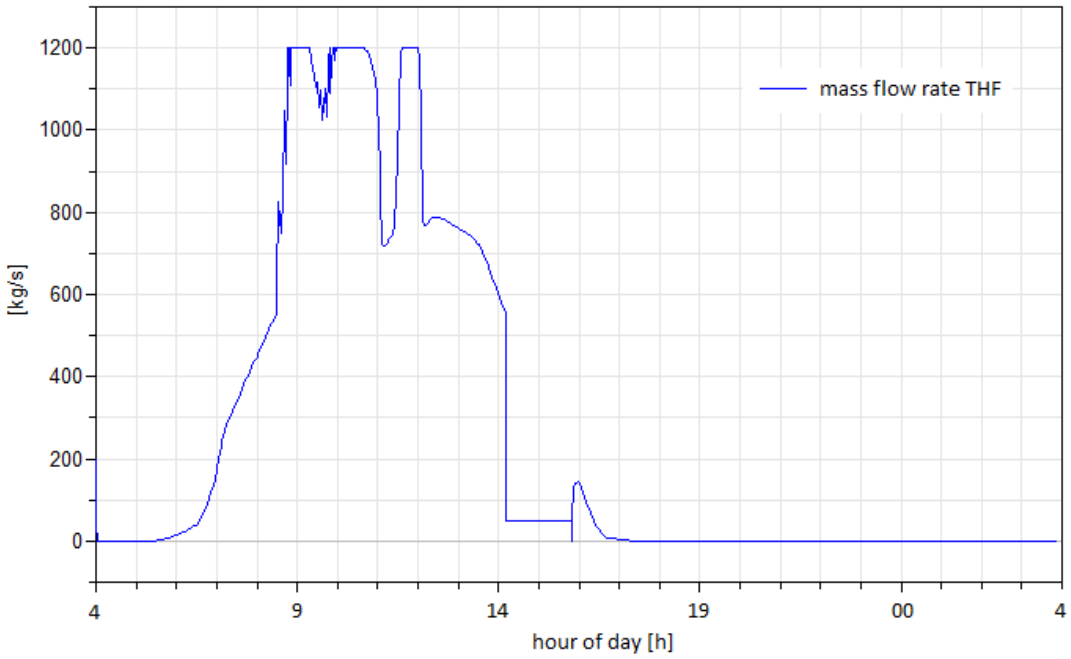

Figure 41 Mass flow rate of thermal heating fluid during the clear autumn day simulation. Simulation starts 4 AM.

In Figure 41 the mass flow rate of thermal heating fluid is shown during the simulation. The heavy fluctuation in mass flow causes the other parts of the control circuit to behave in the same way which makes the simulation go very slow and deliver bad results. Even though the feed forward control design for the thermal heating fluid pump is chosen to prevent this kind of behavior it doesn't manage to control the system in a very good way.

9.5 CLEAR WINTER DAY

To investigate how well the system performs on a winter day a simulation was run on day 358 that is the 24th of December. Surprisingly the incoming solar irradiation at this time of the year is high enough for the system to run the Rankine cycle and charge the thermal storage as seen in Figure 43. The sun goes down earlier this time of year shown in Figure 42 compared to the results from the clear summer day in Figure 31. Compared to the solar irradiation for the clear spring day in Figure 36 the solar irradiation for the winter day is even higher. The reason for this can be that the day chosen for the spring simulation has a history of very low solar irradiation or the weather is generally worse during spring than winter at the location.

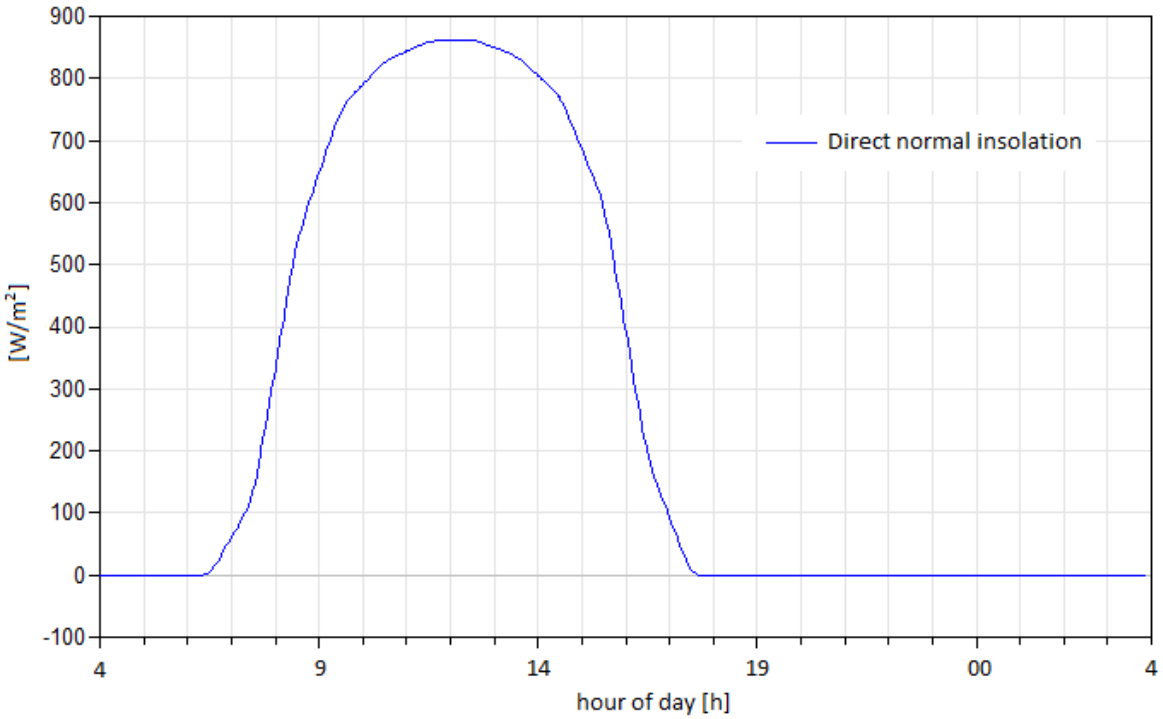

Figure 42 Direct normal irradiation during the clear winter day simulation. Simulation starts 4 AM.

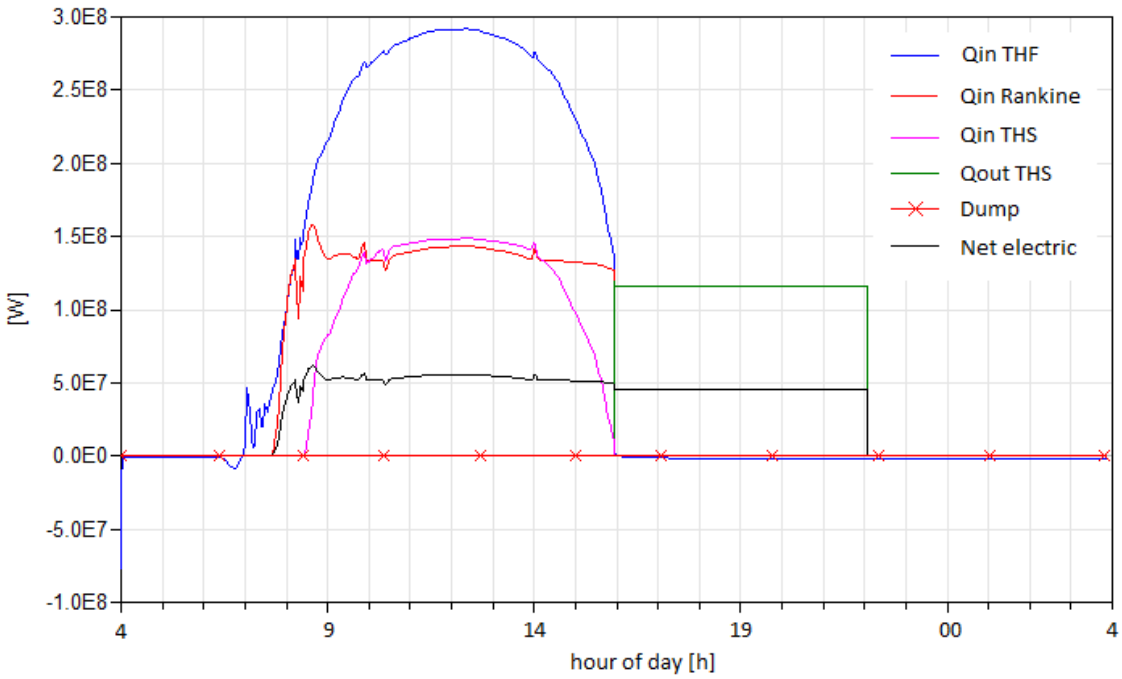

Figure 43 Heat flow to and from system parts for the clear winter day simulation. Simulation starts 4 AM.

10 DISCUSSION AND CONCLUSIONS

10.1 DISCUSSION

The goal with this master thesis was to successfully simulate a concentrating solar power plant of some type. The type chosen, parabolic trough is the most common type at the moment and has a huge potential to deliver large amount of environmental friendly electricity. In order to model other types of concentrating solar power plant the current models may be redesigned rather easily for linear Fresnel. A central receiver design is so very different from these two types of power plants that it's not possible to reuse the models in an easy way. For this type system a new set of models would have to be developed.

The final results presented may not be very useful in its current form but the models developed could be used for research and future plant development. There is some code already developed for dynamic simulations of parabolic trough solar power plants for the TRNSYS platform. This platform is old and do not offer as high grade of flexibility as the system developed for Dymola. The models for Dymola can easily be altered and customized for a specific plant design and shortens the project development time in the initial project phase where simulations are a big part in the final power plant design. If systems can be modeled with a high grade of accuracy the time from project start to plant startup can be shortened and the plant performance predicted on an early stage. This will probably lead to a more problem free plant startup in the end. New system design can be tested and evaluated in an early stage in Dymola and less physical prototype tests have to be done which is much more cost effective and leads to cheaper plant development cost.

The steady state model validations that were done on the solar model and the collector model show good results that indicate that a correct implementation of the rather tricky loss models was made.

These models are ready to use for system simulations. The thermal storage needs more work in order to be ready to use and the model implemented at the moment is too simplified.

Because of time shortage no Rankine cycle was implemented which of course is a pity but the overall results presented in Figure 32 compared to the graph provided by Flabeg in Figure 30 show strong similarities.

The fast switching between states, charging and dis-charging the thermal storage, could be avoided with better automatic control circuits. The fluctuations in the beginning of the simulations could also be avoided if a better control circuit was used. The automatic control circuit has to be optimized for each simulation depending on how much solar irradiation is hitting the collector during the day. The effects of this have to be studied more carefully to gain knowledge of which control parameters to change and how much depending of the solar irradiation.

A lot of work was put down on the automatic control circuit but it is still not working as well as wanted. More expertise and knowledge about automatic control structure is needed in order to develop a better and more efficient one for a future system.

Working with Dymola is a bit of a challenge in the beginning before one get to know the software suit better. But in the end it's a very powerful simulation tools and can be used for like in this case thermal power plant simulations.

Looking back on the work a little too much time was spent on working with the simple system in Dymola. The time spent on this was a big part in learning the software suite but very little of the work done was to any use when a more complete system was developed. A faster switch to development of the models that was to be used and validated should have been done.

10.2 CONCLUSIONS

The models developed are mostly solid and show good results in steady state modeling.

The thermal storage is simplified and needs more work.

No real Rankine cycle lowers the total impression of the work.

Hard to validate the models but are validated as good as possible with available data.

The final results from simulations aligns well with the predicted result.

The automatic control circuit needs improvement.

11 FUTURE WORK

A complete and working Rankine cycle for more accurate performance simulations.

More advance and real like thermal storage model.

More optimized control circuit adapting to changes in amount of solar irradiation between different simulations.

Ability to dump, defocus a part of the solar field, when thermal storage is not completely fully charged.

Better modeling of thermal inertia to avoid fast switched between model states like charging and discharging.

12 REFERENCES

[1] P. Menna och D. Rossetti, ”Concentrating solar power - from research to implementation,” Office for official Publications of the European Communities, Luxembourg, 2007.

[2] W. Stine och M. Geyer, ”Chapter 11 - Energy storage,” 29 10 2013. [Online]. Available: http://www.powerfromthesun.net/Book/chapter11/chapter11.html.

[3] W. Stine och M. Geyer, ”Chapter 12 - Power Cycles for Electricity Generation,” 29 10 2013. [Online]. Available: http://www.powerfromthesun.net/Book/chapter12/chapter12.html.

[4] ”Shams 1 factsheet,” 29 10 2013. [Online]. Available: http://www.shamspower.ae/resources/media/Factsheet-ShamsFlyerEnglish.pdf.

[5] ”Technology Characterization Solar Parabolic Trough,” 29 10 2013. [Online]. Available: http://www.solarpaces.org/CSP_Technology/docs/solar_trough.pdf.

[6] A. Farzaneh, M. Mohammadi och Z. Ahmad, Aluminium Alloys in Solar Power - Benefits and Limitations, Intech Open Science, 2012.

[7] ”Technology Characterization Solar Power Towers,” 29 10 2013. [Online]. Available: http://www.solarpaces.org/CSP_Technology/docs/solar_tower.pdf.

[8] ”Ivanpah solar project,” 29 10 2013. [Online]. Available: http://www.brightsourceenergy.com/ivanpah-solar-project.

[9] ”Technology Characterization Solar Dish Systems,” 29 10 2013. [Online]. Available: http://www.solarpaces.org/CSP_Technology/docs/solar_dish.pdf.

[10] M. Gunther, ”Linear Fresnel Technology,” i *Advanced CSP Teaching Materials*, Enermena;Deutsches Zentrum fur Luft- und Raumfahrt.

[11] ”Concentrating Solar Power Projects by Country,” 29 10 2013. [Online]. Available: http://www.nrel.gov/csp/solarpaces/by_country.cfm.

[12] L. Friedman, ”Can North Africa Light Up Europe With Concentrated Solar Power?,” 20 June 2011. [Online]. Available: http://www.nytimes.com/cwire/2011/06/20/20climatewire-can-north-africa-light-up-europe-with-concen-79708.html?pagewanted=all.

[13] W. Stine och M. Geyer, ”Solar Energy System Design,” 29 10 2013. [Online]. Available: http://www.powerfromthesun.net/Book/chapter01/chapter01.html.

[14] ”Gemasolar plant description,” 06 06 2010. [Online]. Available: http://www.torresolenergy.com/TORRESOL/gemasolar-plant/en. [Använd 29 10 2013].

[15] ”Andasol-2,” 29 10 2013. [Online]. Available: http://www.nrel.gov/csp/solarpaces/project_detail.cfm/projectID=4.

[16] ”Prabolic Trough Projects,” 29 10 2013. [Online]. Available: http://www.nrel.gov/csp/solarpaces/parabolic_trough.cfm.

[17] Eastman Chemical Company, ”Therminol VP-1 product description,” 28 10 2013. [Online]. Available: http://www.therminol.com/pages/products/vp-1.asp.

[18] T. Bauer och N. Breidenbach, ”Overview of molten salt storage systems and material development for solar thermal power plants,” DLR, Köln,Germany.

[19] Eastman Chemical Company, ”Therminol VP-1 product information,” 28 10 2013. [Online]. Available: http://www.therminol.com/pages/bulletins/therminol_vp1.pdf.

[20] R. Ferri, A. Cammi och D. Mazzei, ”Molten salt mixture properties in RELAP5 code for thermodynamic solar applications,” *International Journal of Thermal Sciences,* pp. 1676-1687, 2008.

[21] J. A. Duffie and W. A. Beckman, Solar engineering of thermal processes, Second Edition, Madison, Wisconsin: John Wiley & Sons, 1991.

[22] J. M. Wagner och P. Gilan, ”Technical manual for the SAM physical trough model,” National Renewable Energy Laboratory, Colorado, 2011.

[23] R. Forristall, ”Heat transfer analysis and modeling of a parabolic trough solar receiver implemented in engineering equation solver,” National Renewable Energy Laboratory - U.S. Department of Energy, Coloroado, 2003.

[24] Y. Xiong, Y. Wu, C. Ma, K. Traore och Y. Zhang, ”Numerical investigation of thermal performance of heat loss of parabolic trough receiver,” *Science China,* pp. 444-452, 5 February 2010.

[25] Schott glass company, ”Schott borosilicate glass product properties,” 28 10 2013. [Online]. Available: http://www.schott.com/borofloat/english/attribute/index.html.

[26] F. Burkholder och C. Kutscher, ”Heat loss testing of Schott's 2008 PTR70 parabolic trough receiver,” National Renewable Energy Laboratory, Golden,Colorado, 2009.

[27] R. Kistner, Interviewee, *Dumping of heat in the Andasol power plant.* [Intervju]. 18 September 2013.

[28] G. Solar, ”Typical Meteorological Year Solar Data From Plataforma Solar de Almeria, Spain,” GeoModel Solar, Bratislava, 2013.

[29] S. S. CSP, ”Schott Solar CSP - PTR70 Receiver information,” 6 June 2013. [Online]. Available: www.schott.com/csp/english/schott-solar-ptr-70-receivers.html. [Använd 6 June 2013].

[30] A. Cobra, ”Andasol 1 Thermo solar energy project information,” [Online]. Available: www.estelasolar.eu/fileadmin/ESTELAdocs/documents/powerplants/Andasol.pdf. [Använd 30 October 2013].

[31] U. Herrmann, M. Geyer och R. Kistner, ”The Andasol Project - workshop on thermal storage for trough power systems,” FLABEG Solar International, Germany, 2002.